A comprehensive overview of conventional and bio-based fillers for rubber formulations sustainability

Materials Today Sustainability 27 (2024) 100886

Contents lists available at ScienceDirect

Materials Today Sustainability

journal homepage: www.journals.elsevier.com/materials-today-sustainability

A comprehensive overview of conventional and bio-based fillers for rubber formulations sustainability

Mehran Dadkhah *, Massimo Messori

Department of Applied Science and Technology (DISAT), Politecnico di Torino, Corso Duca Degli Abruzzi 24, 10129, Torino, Italy

ARTICLE INFO

Keywords:
Sustainability
Rubber
Composites
Bio-based filler

ABSTRACT

In recent years, there has been a significant increase in literature regarding the development of sustainable rubber composites. This is due to the widespread use of rubber and the need to transition towards a circular economy, which addresses environmental concerns such as global warming and pollution. Extensive research has been conducted to replace conventional fillers like silica and petroleum-based fillers in rubber composites with eco-friendly and sustainable alternatives, namely bio-based fillers. These biofillers present diverse fundamental characteristics, making them promising substitutes for carbon black or inorganic mineral-based fillers, reducing reliance on petroleum. They possess biodegradable properties, resulting in a reduced environmental footprint, as well as lower density and cost compared to conventional counterparts. Furthermore, their unique properties, such as high specific strength and stiffness, render them well-suited for various rubber applications. The performance of reinforced rubber composites is influenced by factors including the matrix polymer, as well as the source, size, shape, chemical composition, and volume fraction of fillers. Rubber composites incorporating biofillers offer the dual advantages of economic efficiency and environmental sustainability. This article provides a comprehensive review of recent research in rubber composite development, with a specific focus on utilizing various fillers. Additionally, it examines the characterization of both conventional and bio-based fillers and their effects on the behaviour and performance of rubber composites, including morphology, thermal properties, and mechanical properties.

1. Introduction

In the present era, rubber-based composites are attracting much attention due to their wide range of applications in various industries, including automotive, aerospace, sports, adhesives, tires, hoses, gloves, O-rings, conveyor belts, fire-proofing materials, footwear etc. [1,2]. One of the critical processes in the rubber industry is vulcanization or curing, which involves cross-linking the rubber chains to form a three-dimensional network structure, resulting in improved performance. Depending on the requirements, during this process, different curing ingredients, such as cross-linking agents, cure activators, accelerators, anti-degradant and plasticizers, are incorporated into the rubber matrix to attain various functionalities in the obtained material [3]. Non-etheless, pure rubbers do not possess the required properties for industrial applications. Therefore, to enhance the processing and mechanical properties of the vulcanizates and introduce new features to rubber, inorganic and insoluble foreign materials, known as fillers, are incorporated into the unfilled rubber system [4]. Fig. 1 displays the different categorizations of fillers [5].

The properties of the fillers, such as particle size, particle shape, specific surface area, volume fraction, aspect ratio, structure, surface chemistry, as well as the interaction between the filler and the matrix, all remarkably contribute to determining the performance of vulcanizates [6]. The spatial arrangement of the filler within the rubber matrix is influenced by factors such as the filler loading, filler activity and its interaction with curatives. In addition, the type of filler, its structure, and its content have a remarkable role in the intensity of interfacial interactions and the overall morphology of the rubber composite. The fillers and vulcanising agents increase the cross-linking between polymer chains and restrict the molecular flow, which improves rubber products' strength and resiliency [7]. Fillers can improve the rubber vulcanizates' reinforcement, modulus, tensile strength, abrasion resistance, and tear strength. They can also enhance the processability and heat resistance of the rubber compounds [8]. Besides, fillers also induce significant inelastic behaviour. When composites undergo stretching from their original state, unloading, and subsequent reloading, the stress

* Corresponding author.
E-mail address: mehran.dadkhah@polito.it (M. Dadkhah).

https://doi.org/10.1016/j.mtsust.2024.100886
Received 5 September 2023; Received in revised form 17 March 2024; Accepted 17 June 2024
Available online 18 June 2024

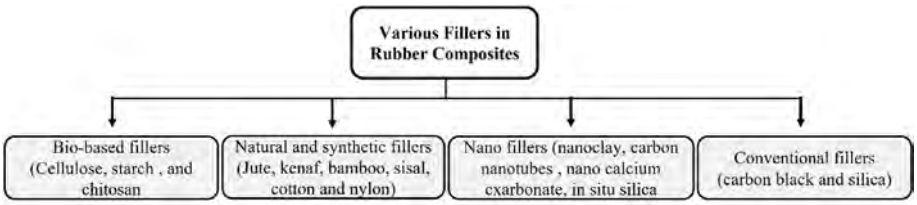

Fig. 1. Categorizing of various fillers in rubber composites.

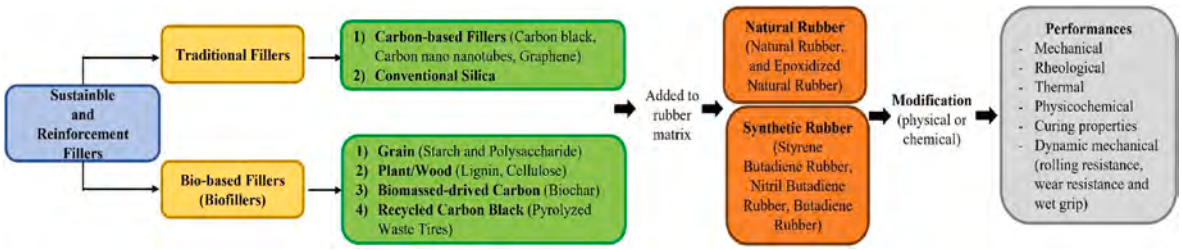

Scheme 1. The total structure and scope of this review paper.

required during reloading is typically lower than that experienced during the initial loading. This phenomenon is known as the Mullins effect, generally attributed to a continuous damage process [7,9]. Non-etheless, the specific damage mechanisms under significant cyclic applied stresses remain incompletely understood. It is believed that the type of filler influences the mechanism of the Mullins effect [10]. This phenomenon is essential in comprehending behaviours such as heat accumulation, failure of rubber products, and mechanical loss during cyclic deformations [11,12].

The choice of filler depends on the desired properties of the final product and its application. Based on the reinforcing effect of fillers on the filled rubber composites, they are categorized into three various groups, as follows [13]:

- Reinforcing fillers with 10–100 nm particle sizes, such as carbon black (CB), silica, graphite, and carbon nanotubes (CNTs), enhance rubber composites' mechanical features.
- Semi-reinforcing fillers with particle sizes of 100–1000 nm, such as hard clay and precipitated calcium carbonate, possess very little ability to improve rubber composites' mechanical characteristics and strength.
- Non-reinforcing fillers with particle sizes of 1000–100000 nm, such as calcium carbonate (dry ground), talc, metal oxide, and barium sulfate, can negatively affect the rubber composites' mechanical properties. Despite this, in the rubber industry, they are incorporated into the rubber compound to reduce production costs.

Incorporating reinforcing fillers into the rubber matrix significantly improves the modulus and other required performance, such as tensile strength and abrasion resistance. Therefore, such fillers attract more attention in various industries, particularly tire manufacturing, where strength, durability, and other performance are essential [14].

In the case of bio-fillers, which are often hydrophilic, their compatibility with non-polar elastomers poses a challenge. To address this, surface modifications of biofillers or compatibilizers have been explored [15,16]. Modifiers enhance the interactions between the rubber matrix and fillers, such as treating the surface of the filler with a coupling agent before incorporating it into the rubber matrix or directly adding a coupling agent to the composite. Silanes, in particular, are commonly used additives to improve the interfacial adhesion and compatibility between fillers and rubber matrix [17].

This review provides an overview of the recent advancements in using sustainable traditional and bio-based fillers in rubber composites. The focus is on their application in natural rubber (NR) and synthetic rubbers such as styrene butadiene rubber (SBA), nitrile butadiene rubber (NBR), and butadiene rubber (BR). The review examines the impact of different fillers on the structural-features relationship of rubber composites. It explores their potential for a partial or complete replacement with CB in various applications. Scheme 1 displays an outline of the review's structure and scope.

2. Traditional fillers in rubber composites

2.1. Carbon-based fillers

Carbonaceous reinforcing materials critically affect the strength and performance of composites. Among them, CB, with >90% of pure form of elemental carbon, is the oldest [18] which is most commonly used in the rubber industry as a sustainable reinforcement filler, especially in the production of tires, including inner liners, sidewalls carcasses, conveyor wheels, air springs, belts, etc. [19]. CB improves the properties of rubber composites, such as tear strength, tensile strength, abrasion resistance, skid resistance, hardness, flexing fatigue, and modulus. Furthermore, adding CB in NR promotes the Payne effect [20]. The characteristics of the final rubber composite can be affected by the properties of CB, such as primary particle size, surface activity, structure, content and its dispersion degree in the rubber matrix [21,22].

Scientists have comprehensively studied the effect of loading, the content of CB, its structure and particle size on the performance of filled rubber composite. Chanda et al. [23] studied the mechanical properties and the fatigue crack growth (FCG) behaviour of filled NR composites containing commercial CB with various particle sizes and structures such as N115, N134, N220, N234, N330, and N339. It was reported that CB with smaller particle size and higher surface area increased NR composites' tensile strength and modulus (M100 and M300) due to better distribution in the matrix with the higher volume interaction between filler and NR rubber. In addition, these composites showed superior FCG resistance than the NR composites filled with the high particle size of CB. Fu et al. [24] prepared grafted carbon black (GCB) using polyethene glycol (PEG) and used it as a filler (up to 60 phr) for reinforcing NR. They compared the mechanical characteristics and Mullins effect of GCB/NR with CB/NR composites. The enhanced compatibility between NR and GCB improved NR's physical and mechanical properties. The study revealed the presence of the Mullins effect in both the unfilled and filled NR composites. The Mullins effect increased with the addition of filler, but the impact varied for CB and

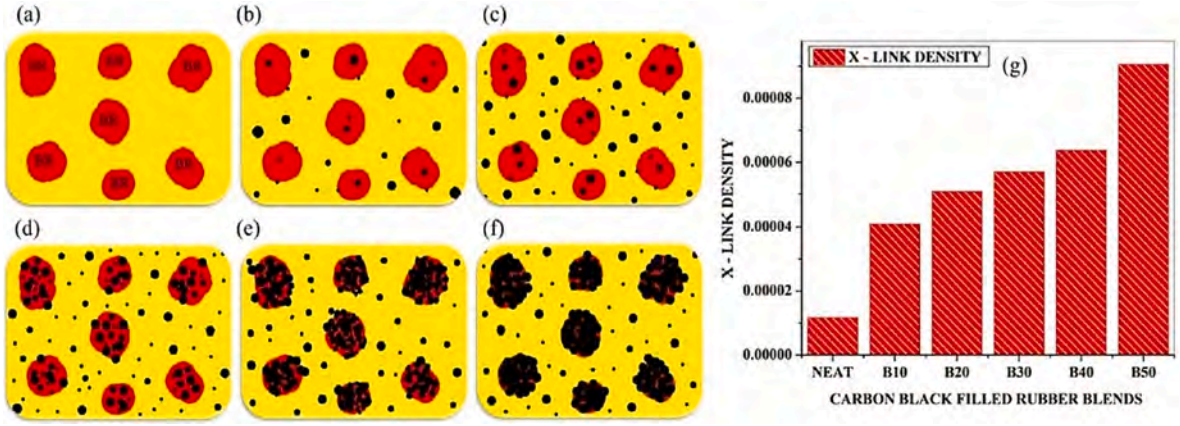

Fig. 2. A schematic of (a) Neat 70NR:30BR RRBs; and filled RRBs with different CB (b) 10 phr; (c) 20 phr; (d) 30 phr; (e) 40 phr; (f) 50 phr, and (g) X–link density, after curing at 150 °C, reprinted from Ref. [28].

GCB. The Mullins effect was stronger in GCB/NR than in CB/NR when the filler addition was below 20 phr. In contrast, when the filler addition exceeded 30 phr, the Mullins effect of CB/NR was stronger compared to GCB/NR. In the NR vulcanizate with low filler content, the Mullins effect should be mainly attributed to the destruction of the filler-rubber interaction during the stretching process. On the other hand, the NR containing high filler content should be principally associated with the destruction of the filler-filler 3D network structure during the stretching process. Moreover, during the high-temperature treatment process, the Mullins effect gradually increased due to the re-entanglement of the rubber molecular chains, the regeneration of the filler-rubber interaction, and the filler-filler 3D network structure. Diaz et al. [25] investigated the physical damage responsible of the Mullins softening in a CB (40 phr) filled SBR. They believed that the layer of bonded rubber at the interface of filler and rubber was crucial in determining the stiffness and Mullins softening of CB filled SBR. In fact, the observed Mullins softening during the initial stretching caused by the desorption of chains from the filler surface. In another study, Li et al. [26] evaluated the Mullins effect of CB filled NBR composites during cyclic tensile deformation. They reported that although the presence of filler at high concentrations significantly retards the mechanical recovery of softening, the Mullins effect is primarily related to the viscoelastic deformation of the rubber phase. These findings indicated that the energy loss associated with hysteretic recovery and softening are determined by the viscoelastic matrix and the filler, respectively.

Recently, Zhou et al. [27] discussed the effect of ionic liquid (IL) on the structure and characteristics of CB-filled NR vulcanizates. It was revealed that the IL accelerated NR vulcanization and promoted CB dispersity. Besides, filled composites' tensile strength and extensibility improved at high filler content. Kaliyathan et al. [28] added various amounts of CB (10–50 phr) to the NR/BR composite (RRBs) to evaluate its effect on the curing and mechanical characteristics of rubber composite. According to DMA analysis, approximately 3.7/10, 8.4/20, 20.7/30, 32/40, and 40/50 CB in filled RRBs composite were partitioned towards BR (Fig. 2b–f). The enhancement in cross-link density with increasing the content of CB can be associated with the physico-chemical adsorption between chains of rubber and the surface of CB, which formed 3D networks (Fig. 2g). Moreover, the presence of curatives caused the formation of chemical cross-links. By incorporating the CB into the RRBs composite, the mechanical features such as modulus values, tensile strength, and tear strength improved compared to neat RRB. On the contrary to RRB, the time value and maximum torque decreased and increased, respectively, for CB-filled RRBs.

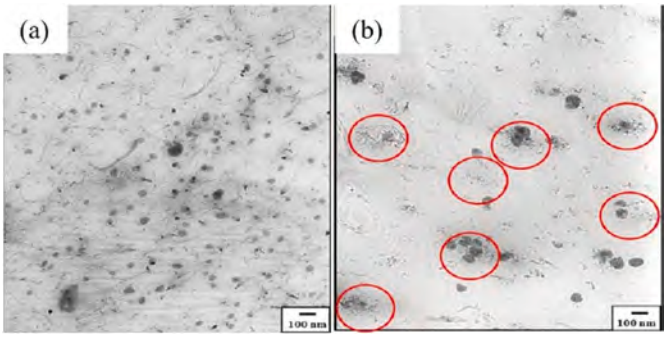

Fig. 3. TEM images of filled epoxidized natural rubber composites with (a) S-MWCNTs; (b) L-MWCNTs, Reprinted from Ref. [36].

Other carbonaceous materials such as graphite, graphene, carbon nanotubes (CNTs), and multi-walled carbon nanotubes (MWCNTs) have received considerable attention owing to their outstanding features, including excellent mechanical, thermal, electrical, and optical characteristics [29]. However, using these materials in composites is still primarily in the experimental and developmental stages, and their applications are currently limited. One of the key advantages of these carbonaceous materials is their ability to provide significant reinforcement even at low loading levels, typically in the range of 1–5 wt% in composites. It contrasts with traditional mineral fillers and fibres that require much higher loadings (up to 50%) to achieve comparable performance. The incorporation of these carbonaceous materials in composites allows for the reduction of filler content, resulting in lighter-weight end products [30].

CNTs are an excellent reinforcing filler in rubber composites due to their superior mechanical and physical features [31]. Compared to conventional fillers like CB, the dispersion of lower concentrations CNTs in the rubber can impart significant reinforcing effects [32]. Xu et al. [33] studied the impact of adding MWCNTs (4 phr) on the morphology and properties of CB/NR composites. They reported an increase in the tensile strength, stress at 300 % strain, tear strength and steady-state thermal conductivity of NR/CB/MWCNTs composites by 12.36%, 26.02%, 16.95% and 102%, respectively, compared to NR/CB composite. Such a finding could be due to the homogenous dispersion of MWCNTs, synergistic reinforcing effect between MWCNTs and CB, and interfacial bonding between carbon nanotubes and the NR matrix. Gu et al. [34] investigated the effect of boron nitride nanosheets (BNNS), CNTs and their hybrid (BNNS-CNT) on the mechanical and thermal performances of SBR nanocomposites. The obtained results showed that the tensile strength of the SBR composites significantly increased to 1.72 $\pm$ 0.24 MPa, 4.09 $\pm$ 0.35 MPa, and 3.37 $\pm$ 0.29 MPa in the presence of 4 phr BNNS, CNTs, and (BNNS-CNT), respectively. Additionally, there was an improvement in the tear strength of SBR to 13.8 kN/m, 16.1 kN/m, and 18.2 kN/m in the presence of 4 phr BNNS, CNTs and (BNNS-CNT)

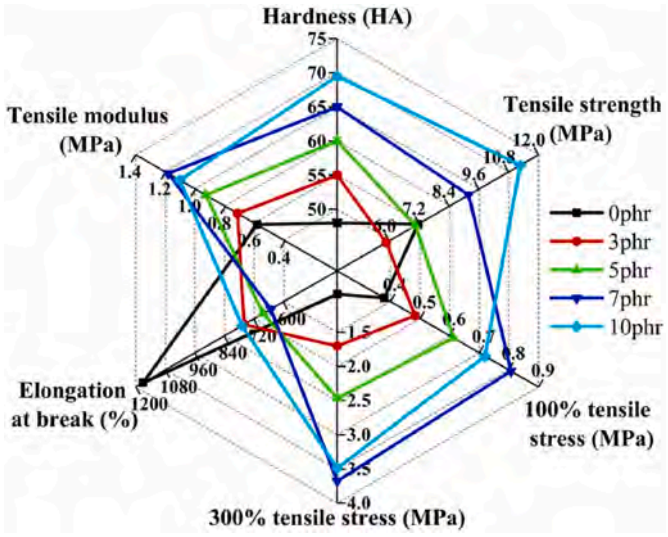

Fig. 4. Basic mechanical characteristics of the CNT/NR composite, Reprinted from Ref. [37].

nanofillers, respectively. Al-Hartomy et al. [35] conducted a study on NR composites containing MWCNTs and graphene nanoplatelets (GNPs) as fillers. They found that the interaction between the NR and filler in the MWCNTs/NR composites was stronger than in GNPs/NR composites. This result showed the better reinforcing effect of carbon nanotubes. Matchawet et al. [36] investigated and compared the curing and mechanical properties of epoxidized natural rubber (ENR) composites comprising long and short MWCNTs and CB as fillers. It was revealed that ENR composites with low-loading short MWCNTs (S-MWCNTs) had similar torque values as the composite with high loading of CB. It could be attributed to the good dispersion and distribution of S-MWCNTs in the ENR matrix (Fig. 3a), which improved rubber chain entanglement and the physical and chemical interactions of fillers and the ENR molecules. On the contrary, the composite with higher loading of long MWCNTs (L-MWCNTs) showed much torque difference concerning S-MWCNTs and CB composites. Besides, L-MWCNTs had poorly distributed and strongly clustered particles (Fig. 3b), leading to higher filler–filler interactions, which agreed well with the highest torque difference. In all filler loading, S-MWCNTs/ENR composites had the highest Young's modulus than L-MWCNTs/ENR composites. It was possibly due to the higher cross-link density and higher content of linkages between epoxide groups in rubber molecules and the polar functional group at the MWCNT surfaces.

Recently, Teng et al. [37] evaluated the adhesion friction behaviours and mechanical properties of NR in the presence of different content of CNTs (3, 5, 7, and 10 phr). As shown in Fig. 4, the addition of CNTs to the NR composite led to the linear increase of hardness and 100% tensile stress, while CNT loading first increased the tensile modulus and then decreased by excessive CNT. By incorporating 7 phr CNT, the hardness, tensile modulus, 100% and 300% tensile stresses were increased by 35.4%, 101.1%, 134.2% and 290.3%, respectively, compared to NR. Moreover, the load-changed real contact area affected the friction coefficient and increased by 23.5%, 27.1%, and 9.2% under 5, 10, and 15 N.

Various studies have been conducted on the effect of graphene and its derivatives as a most promising reinforcing filler on the performance of rubber composite due to its favourable feature, including high Young's modulus, thermal conductivity, specific surface area and intrinsic mobility [38,39] Non-etheless, homogeneous dispersion of graphene in rubber matrix remains a big issue, and using modification forms of graphene can avoid it, such as graphene oxide (GO) and reduced graphene oxide (rGO) [40]. Kang et al. [41] used reduced graphene oxide to develop graphene/NR nanocomposites by simple mechanical mixing. By the addition of 2 phr graphene, the tensile strength received to maximum and increased by approximately 17% with respect to pure NR. It can be attributed to the large specific surface area and better withstanding of the external force of graphene as a nanofiller. However, more addition of graphene formed agglomeration and deteriorated the tensile strength. Furthermore, the elongation at the break of filled NR nanocomposites decreased by increasing graphene loading because of the restricted movement of polymer chains. Recently, An et al. [42] prepared functionalized graphene oxide using a simple, green, one-step hydrothermal method by water-soluble 2-mercapto-1--methylimidazole (MMI). The modified filler (GO-MMI) could be evenly dispersed in the NR matrix using mechanical blending. The obtained GO-MMI/NR composites showed good comprehensive features due to the improved interfacial interaction between GO-MMI and NR matrix, which makes them a promising candidate for industrial-scale green tires. In comparison with unmodified GO/NR composites, the elongation at break (801%), low heat build-up (6.2 °C), tensile strength (26.8 MPa), Deutsches Institute for Normung (DIN) abrasion loss volume (71.31 mm^3) and heat resistance index (162.1 °C) of GO-MMI/NR composite were synchronic-lifting.

Liu et al. [43] developed a new hybrid filler from SiO_2 nanoparticles (NSi) decorated with reduced graphene oxide (GSi) for application in green tires. It was found that the tensile strength, elongation at break and heat resistance index of GSi/NR composite increased up to 27.5 MPa, 507% and 182.2 °C, respectively, which can be due to the excellent dispersion of GSi in the rubber matrix. In another study, Li et al. [44] prepared GO@SiO_2 hybrid filler using a silane coupling agent and an in-situ generation method. Because of the presence of amino and epoxy groups on the surface of these hybrid fillers, they were used as reactive compatibilizers for improving interfacial compatibility and cross-link density with SBR/NR latex (SBR/NRL) composites. Besides, the dispersion of GO@SiO_2 filer in the rubber matrix was uniform, and there was a significant improvement in the mechanical features and wet skid resistance of composites. The filled SBR/NRL composites with the mass ratio of GO to SiO_2 = 3:10 showed an increase in the tensile strength, tear strength, wear resistance and wet skid resistance by 96.7%, 73.7%, 20.6%, and 21.9%, respectively compared to the composite filled with only SiO_2. Based on these results, the authors proposed the broad application of these composite in "green tire."

Several authors have also reported attempts for partial and full replacement of CB with other carbonous materials without compromising the properties of the final composite formulations. Bijina et al. [45] proposed an eco-friendly, green tyre tread formulation with excellent abrasion resistance, rolling resistance, mechanical feature and heat buildup properties by partially replacing CB with graphite. The formulation with 10 phr thermally exfoliated graphite increased the tensile, tear and abrasion performances by 11%, 10%, and 18%, respectively, concerning the standard formulation with a nominal amount of CB filler. It was possibly due to the high surface area of graphite, which formed a good interaction between the filler and rubber matrix [46]. Moreover, the rolling resistance and heat build-up were significantly reduced by 45% and 53%, respectively, compared with the standard formulation. Rajan et al. [47] studied the partial replacement of CB with various amounts of modified graphene (1, 2.5 and 5 phr) in the NR/BR matrix. They reported the formulation with 2.5 phr of graphene as the optimum replacement concentration. The results showed an increase in elongation at break and the bound rubber content of filled composites attributing to an effective interaction between the rubber and the modified graphene. Furthermore, partially replacing CB with modified graphene decreased the rolling resistance, making it favourable for developing sustainable green tyre compounds. Innes et al. [48] assessed the reinforcement characteristics of graphene nanoplatelets (GNPs) as a replacement for CB in a NBR matrix. The results showed that the tensile strength and tear features of GNPs/NBR composites increased, whereas curing times and scorch times were smaller and longer, respectively, compared to CB/NBR composites. Such a finding

Table 1
Mechanical properties of rubber composites containing various carbon-based fillers (CNTs, CB, Graphene or its derivatives, and hybrid fillers).

Rubber composites		Filler loading	Mechanical characteristics	Modifier	Ref
CNTs Fillers	CNTs/ENR-$FeCl_3$	Unfilled ENR (control)	- Tensile strength (MPa): 1.89 ± 0.11 – 100% Modulus (MPa): 0.89 ± 0.18 - Hardness (∘ Sh A): 44.5 ± 1.0	–	[49]
		CNTs: 10 phr	- Tensile strength (MPa): 2.81 ± 0.43 – 100% Modulus (MPa): 1.75 ± 0.18 - Hardness (∘ Sh A): 76.6 ± 2.0		
	CNTs/SBR	Unfilled SBR (control)	- Tensile strength (MPa): 2.9 – 200% Modulus (MPa): 1.4 - Elongation at break (%): 380 - Toughness (MJ/m^3): 5.5	–	[50]
		CNTs: 3 wt%	- Tensile strength (MPa): 5.2 – 200% Modulus (MPa): 3.0 - Elongation at break (%): 384 - Toughness (MJ/m^3): 10.9	Functionalized CNTs	
	CNTs/NR latex	CNTs: 5 phr	- Tensile strength (MPa): 18.3 ± 0.72 – 100% Modulus (MPa): 2.3 ± 0.18 - Elongation at break (%): 595 ± 17.7	Silane	[51]
	CNTs/ENR	CNTs: 5 phr	- Tensile strength (MPa): 8.2 ± 0.5 – 100% Modulus (MPa): 2.2 ± 0.1 - Elongation at break (%): 366 ± 19.9	(APTES)	[52]
			- Tensile strength (MPa): 21.5 ± 1.9 – 100% Modulus (MPa): 4.7 ± 0.5 - Elongation at break (%): 576 ± 34.0	(TESPT)	
	MWCNTs/NR/SBR	MWCNTs: 2.5 phr	- Tensile strength (MPa): 26.2 - Tear strength (kN/m): 62.7 - Elongation at break (%): 436 - Akron abrasion loss (cm^3):0.1129	Organically functionalized MWCNTs	[53]
	MWCNTs/NBR	MWCNTs: 5 phr	- Tensile strength (MPa): 4.83 ± 1.0 – 300% Modulus (MPa): 1.74 ± 0.3 - Elongation at break (%): 752 ± 6	–	[54]
Graphene filler or its derivatives	GO/NR	GO: 5 phr	- Tensile strength (MPa): 16.55 ± 0.34 – 300% Modulus (MPa): 5.71 ± 0.23 - Tear strength (KN/m): 26.01 ± 0.37	–	[55]
			- Tensile strength (MPa): 28.94 ± 1.50 – 300% Modulus (MPa): 11.15 ± 0.34 - Tear strength (KN/m): 51.36 ± 0.42	Polyvinylpyrrolidone (PVP)	
	GO/NR	GO: 5 wt%	- Tensile strength (MPa): 1.17 ± 0.18 - Elongation at break (%): 688 ± 11	–	[56]
	GO/NR	GO: 0.5 phr	- Tensile strength (MPa): 26.8 - Heat build-up (°C): 6.2 - Elongation at break (%): 801 - DIN abrasion loss (mm^3): 71.31	(MMI) Functionalized GO	[42]
	GNPs/NBR	GNPs: 25 phr	- Tensile strength (MPa): 14.69 ± 0.7 – 300% Modulus (MPa): 6.26 ± 0.3 - Elongation at break (%): 768 ± 14	–	[54]
	GNPs/ABS	Unfilled ABS (control)	- Elastic modulus (GPa): 2.147 ± 118 - Yield stress (MPa): 39.0 ± 0.5	–	[57]
		GNPs: 8 wt%	- Elastic modulus (GPa): 2.527 ± 177 - Yield stress (MPa): 40.4 ± 2.5		
	rGO/SBR	rGO: 3 wt%	- Tensile strength (MPa): 4.6 – 200% Modulus (MPa): 2.8 - Elongation at break (%): 370 - Toughness (MJ/m^3): 9.4	–	[50]
	rGO/CR	rGO: 0.9 phr	- Tensile strength (MPa): 12.41 ± 0.33 – 300% Modulus (MPa): 1.58 - Hardness (∘ Sh A): 46 ± 2 - Elongation at break (%): 1250 ± 3.1 - Tear strength (kN/m): 31.36 ± 1.2	–	[58]
Carbon black fillers	CB/NR/BR/SBR	Unfilled BR/SBR (control)	- Tensile strength (MPa): 1.5 - Modulus 100% (MPa): 0.86 - Hardness (∘ Sh A): 37 - Elongation at break (%): 197.5	–	[59]
		CB: 80 phr	- Tensile strength (MPa): 17.2 – 100% Modulus (MPa): 5.71 - Hardness (∘ Sh A): 73 - Elongation at break (%): 254.9		
	CB/NR	CB: 40 phr	- Tensile strength (MPa): 19.8 ± 1.2 – 300% Modulus (MPa): 7.18 ± 0.2 - Hardness (∘ Sh A): 70.8 ± 0.4 - Elongation at break (%): 7.1 ± 0.4 - Bound rubber content (%): 30.0	–	[60]
	CB/NBR	CB: 25 phr	- Tensile strength (MPa): 15.91 ± 1.8 – 300% Modulus (MPa): 2.52 ± 0.2 - Elongation at break (%): 1130 ± 16	–	[54]

(*continued on next page*)

Table 1 (*continued*)

Rubber composites		Filler loading	Mechanical characteristics	Modifier	Ref
Hybrid fillers	CNTs-rGO/SBR	CNTs-rGO: 3 wt%	- Tensile strength (MPa): 8.8 – 200% Modulus (MPa): 7.7 - Elongation at break (%): 230 - Toughness (MJ/m^3): 10.7	Functionalized CNTs	[50]
	CNTs/SiO_2/SSBR/BR	CNTs: 6 wt%	- Tensile strength (MPa): 23.6 - Elongation at break (%): 603.9	–	[61]
	MWCNTs/rGO/CR	rGO: 0.9 phr MWCNTs: 0	- Tensile strength (MPa): 12.41 ± 0.33 – 300% Modulus (MPa): 1.58 - Hardness (∘ Sh A): 46 ± 2 - Elongation at break (%): 1250 ± 3.1 - Tear strength (kN/m): 31.36 ± 1.2	–	[58]
		rGO: 0.9 phr MWCNTs: 4 phr	- Tensile strength (MPa): 10.09 ± 0.60 – 300% Modulus (MPa): 5.65 - Hardness (∘ Sh A): 54 ± 1 - Elongation at break (%): 603 ± 3.1 - Tear strength (kN/m): 66.25 ± 2	–	
	GNPs/CB/NBR	GNPs: 15 phr CB: 10 phr	- Tensile strength (MPa): 20.10 ± 0.8 – 300% Modulus (MPa): 5.22 ± 0.1 - Elongation at break (%): 1055 ± 7	–	[54]
	GNPs/MWCNTs/NBR	GNPs: 15 phr MWCNTs: 5 phr	- Tensile strength (MPa): 15.33 ± 1.3 – 300% Modulus (MPa): 5.26 ± 0.2 - Elongation at break (%): 842 ± 16	–	
	CB/Gr/NR/BR	CB: 55 phr (control)	- Tensile strength (MPa): 24.68 – 300% Modulus (MPa): 11.29 - Hardness (∘ Sh A): 66 - Elongation at break (%): 546	–	[47]
		CB: 52.5 phr Gr: 2.5 phr	- Tensile strength (MPa): 24.77 – 300% Modulus (MPa): 10.1 - Hardness (∘ Sh A): 62 - Elongation at break (%): 621	Functionalized graphene	
	CB/GNPs/NR	CB: 35 phr GNPs: 5 phr	- Tensile strength (MPa): 21.3 ± 1.2 – 300% Modulus (MPa): 7.57 ± 0.2 - Hardness (∘ Sh A): 74.2 ± 0.7 - Elongation at break (%): 7.8 ± 0.4 - Bound rubber content (%): 32.7	–	[60]

CNTs: Carbon nanotubes; **MWCNTs**: Multiwalled carbon nanotubes; **GO**: Graphene oxide; **Gr**: Graphene; **GNPs**: Graphene nanoplates; **$FeCl_3$**: Ferric chloride; **ENR**: Epoxidized natural rubber; **SSBR**: Solution-polymerized styrene-butadiene rubber; **SBR**: Styrene-butadiene rubber; **BR**: Butadiene rubber; **NR**: Natural rubber; **CR**: Polychloroprene rubber; **NBR**: acrylonitrile butadiene; **ABS**: Acrylonitrile–butadiene–styrene; (**TESPT**): bis(triethoxysilylpropyl) tetrasulfide; (**APTES**): 3-aminopropyltriethoxysilane; **DIN**: Deutsches Institute for Normung; (MMI): 2-mercapto-1-methylimidazole.

could be due to the inherent characteristics of GNPs and their geometry, which produce a rubber compound with better performance in the application with higher flexibility, tear strength and compliance. Table 1 presents the main important mechanical characteristics of filled rubber composites with carbon-based fillers.

2.2. Conventional silica filler

Silica is a versatile and durable material, one of Earth's most abundant minerals due to the fact that Silicon is the second most abundant element. Its characteristic properties, such as hydrophilicity, low toxicity, thermal stability, and an easy synthetic route, contribute to its wide-ranging applications [62,63]. It is considered a bonding agent and an excellent sustainable reinforcement material as an alternative for CB in tires [64,65]. The crystalline type of silica often does not possess reinforcing features, while amorphous silica (precipitated and fumed) offers reinforcing properties. Although fumed silica has the smallest particles than the precipitated form of silica, it not generally uses in the tire industry due to processing problems and high costs. For these reasons, precipitated silica is usually used in the tire industry [66].

The introduction of silica as a partial replacement for CB was first offered by Michelin in 1992 to develop "greener tires" [67]. The green term refers to the fact that silica enhances fuel efficiency (3–15%) and reduces rolling resistance (20–30%) in tires which causes lower CO_2 emission into the environment compared with those containing only CB as filler [68].

The rubber manufacturing industry focuses on certain performance factors, including rolling resistance, wear or abrasion resistance and wet grip, commonly known as magic triangle parameters. The fine-tuning of these three parameters is hard in the case of many practical formulations since the enhancement of one factor causes a deterioration of the other [3]. It is obvious from Fig. 5 that the replacement of CB with silica develops high-performance green tires through improved wet grip (enhanced driving safety) and low heat build-up [64,69]. In contrast, it has a negative effect on abrasion resistance (durability) [13].

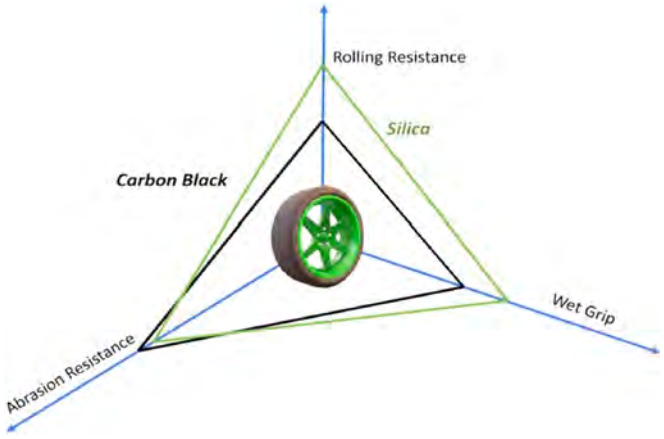

Fig. 5. The performance comparison between silica and CB reinforced rubber (Magic triangle), Reprinted from Ref. [13].

Although silica offers several advantages, its weaker polymer-filler interaction provides fewer reinforcing properties than CB. Using silica in high-performance applications (such as tires) poses specific

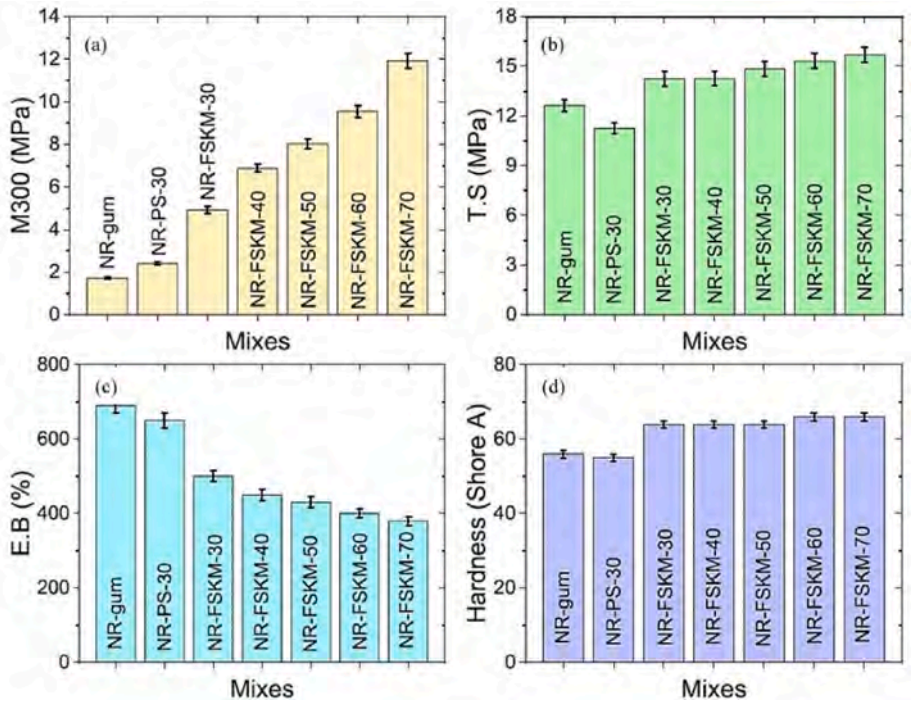

Fig. 6. Mechanical characteristics of NR composites in the presence of precipitated silica (NR-PS-30) and various FSKM loading, (a) Modulus at 300%; (b) tensile strength; (c) elongation at break; (d) hardness, Reprinted from Ref. [75].

challenges regarding optimal dispersion, potential high heat generation, temperature sensitivity, and the tendency for gel formation during the mixing process [70]. The dispersion capacity of silica and its interface strength with rubber matrix significantly affect the characteristics of the final product [71]. In fact, due to inherent polarity differences between silica and rubber matrix, it is difficult to establish strong interaction between the silica particles and a non-polar rubber. Moreover, the presence of highly polar silanol groups on the surface of silica leads to strong interactions between silica particles, making it challenging to achieve proper dispersion in non-polar rubbers and sufficient interfacial compatibility. These polar silanol groups also form hydrogen bonding with polar substances, particularly amine-based accelerators, resulting in the adsorption of curing agents onto the silica surface and slowing down the vulcanization process. However, the surface modification of silica before mixing can overcome these challenges, such as the addition of a silane coupling agent (as reinforcement modifier) in silica-reinforced rubber composite that improves the bonding and interfacial compatibility between the silica surface and the rubber matrix.

Wang et al. [72] prepared silica-NR composites by Si69 (a silane coupling agent) and NR latex (NRL) treatment to solve the problems of high filling, difficult mixing, and easy aggregation. The NRL-treated silica (NRL-Silica) exhibited favourable characteristics like good dispersion and compatibility with rubber. Compared with dry mixing technology, the 100% and 300% tensile modulus increased by 8.5% and 14.47%, respectively, whereas heat build-up decreased by 41.88%. Meantime the obtained composite had a weaker Payne effect, higher wet-skid resistance, and lower rolling resistance, making them suitable for various applications like tire manufacturing. Sengloyluan et al. [73] used bis 3-(triethoxysilyl) propyl tetrasulfide (TESPT) and 3-octanoylthio-1-propyltriethoxysilane (NXT)-grafted NR as the compatibilizer for silica/NR compounds. The results indicated that the NXT-grafted NR had better compatibility than directly using the same amount of silane to improve the tensile properties of NR/silica composites. Despite this, the tensile properties of NR/silica composites were superior in the presence of TESPT concerning NXT-grafted NR. Maciejewska et al. [74] studied the effect of nanosized silica and ionic liquids (ILs) on the physico-chemical, mechanical properties and curing characteristics of the obtained vulcanizates. The addition of nanosized silica in NR compounds noticeably increased the optimal vulcanization time with respect to unfilled NR. Furthermore, incorporating ILs into NR compounds affected the vulcanization process by accelerating the vulcanization rate and contributing to higher cross-link density in NR composites. As a result, vulcanizates' tensile strength and hardness remarkably enhanced compared to those with no ILs. In recent research, Alam et al. [75] explained the reinforcing abilities of (TESPT) functionalized

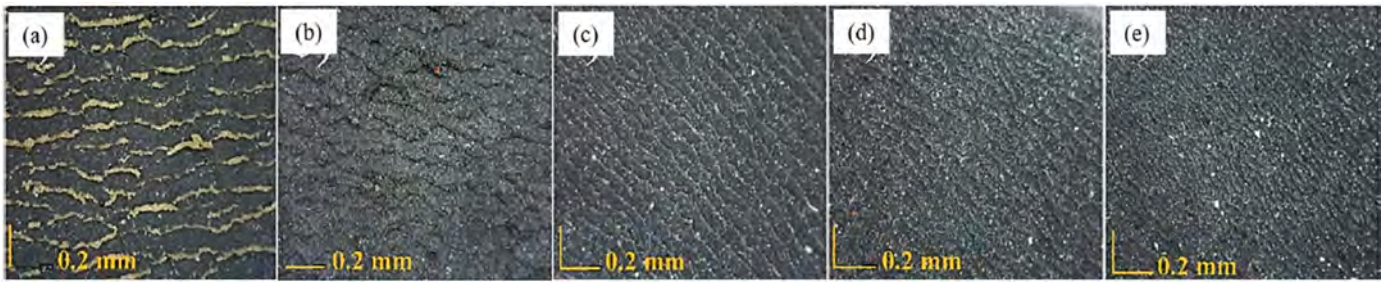

Fig. 7. The effect of incorporating rGO into the silica/SBR composite on the abrasion pattern of the abraded surface, (a) reference composite (0 phr); (b) 0.25 phr; (c) 0.5 phr; (d) 0.75 phr; and (e) 1 phr, Reprinted from Ref. [76].

Table 2
Main features of conventional and bio-based fillers used in rubber composites.

Filler		Density (g/cm^3)	Modulus (GPa)	Surface area (m^2/g)	Properties
Traditional fillers	Carbon black (CB)	1.8–2.1	4–30	7–12	Good mechanical characteristics and abrasion resistance
	Silica	~2.65	60–80	110–240	Good mechanical and thermal features
Bio-based fillers	Biochar	~1.3–1.4	10–25	438 (Pyrolyzed at 600 °C)	High surface area
	Cellulose nanocrystals (CNC)	~1.5	70–134	400–500	Heat stability, high mechanical strength with a high aspect ratio
	Chitin	~1.43	150	360	Biocompatible, biodegradable, and non-toxic
	Lignin	~1.3–1.4	4	15.8 ± 2.5	Abundant and hydrophobic
	Starch	1.5	2.7	0.9–1.3	Biodegradability, non-toxicity, and low cost

silica-kaolinite mineral (FSKM) in NR composite formulations. As can be seen in Fig. 6a, the modulus at 300% (M300) significantly increased in a rubber composite filled with 70 phr FSKM regarding unfilled rubber (NR-gum) and precipitated silica/NR composite (NR-PS-30). Moreover, higher tensile strength (Fig. 6b), shorter elongation at break (Fig. 6c), and higher hardness (Fig. 6d) in the FSKM/NR composites suggested that the filler particles effectively bind to the rubber chains and restrict their movements. In addition to the excellent filler-rubber interactions, better filler dispersions in NR composites resulted in increased mechanical properties and aging resistance of the composite.

Gao et al. [70] proposed a new reinforcing agent, namely, nanocarbon-coated silica (SN), using high-temperature pyrolysis of polyethene. The experimental results showed that the hydroxyl groups on the surface of SN disappeared, and the obtained SN/rubber composites had better electrical conductivity, shorter curing time, and improved dynamic mechanical and thermal properties, making them suitable for high-performance tire applications. Recently Kalat et al. [76] conducted a study on the role of rGO as a secondary filler on the performance of silica/SBR composites. Incorporating a small amount of rGO (0.25 or 0.5 phr) into the SBR composites reduced network formation in unmodified silica and reduced the Payne effect and corresponding energy dissipation. The addition of rGO improved the dispersion of unmodified silica owing to the improvement of interaction between silica-rubber, which occurred during mixing and/or reduced silica flocculation after mixing. Moreover, the mechanical strength and abrasion resistance increased by 45% and 63%, respectively, while heat build-up decreased by 23% due to the synergy between silica and rGO. The abrasion pattern (Fig. 7a) shows large ridges in the reference composite without rGO, indicating a high rubber abrasion. In contrast, the height and spacing between these ridges decreased in the presence of rGO (Fig. 7b–e), exhibiting the reduction of abrasion loss [68]. Therefore, they suggested this hybrid system as an alternative to silane modification for silica in the green tire industry.

3. Towards environmentally friendly sustainable fillers

NR, SBR, and BR, which are major components in tire manufacturing, traditionally rely on synthetic polymers derived from fossil-based raw materials [3]. Besides, CB is commonly used as a reinforcing filler in rubber composites. Since CB derives from petroleum sources, its energy-consuming production and processing lead to environmental pollution [77]. The manufacturing process of CB involves the combustion of hydrocarbon fuels, which can release greenhouse gases and other pollutants into the atmosphere. Furthermore, the handling and disposing of CB during the production and use of rubber composites can also present environmental concerns [78].

With growing global environmental awareness and the aim of reducing environmental pollution and global warming, extensive research has been conducted to replace the existing petroleum-based fillers in rubber composite with eco-friendly and sustainable alternatives using biomaterials. These bio-based fillers produce from renewable sources such as animal (chitosan and chitin), grain (starch and polysaccharide), plant/wood (lignin, cellulose and natural fibre), agricultural waste and industry by-product [79,80]. These bio-based fillers present diverse fundamental characteristics, making them promising candidates to replace CB or inorganic mineral-based fillers. These materials are renewable and biodegradable, contributing to environmental sustainability. They also have a lower density and cost than conventional fillers like CB and silica. Moreover, they possess unique properties such as high specific strength and stiffness, enhancing their suitability for rubber applications [81]. Therefore, using these bio-based fillers in the rubber industry would reduce its reliance on fossil-based resources and contribute to the conservation of the global environment. Table 2 shows the main characteristics of conventional and bio-based fillers that can be utilized in rubber composite [3].

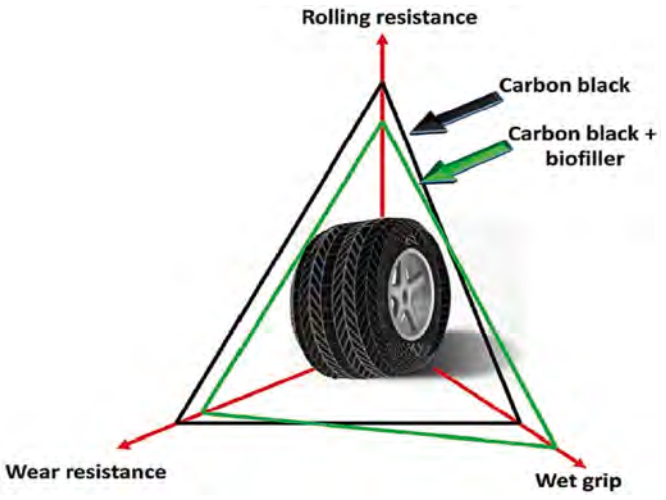

Fig. 8. The comparison of the performance between (CB + bio-filler) and CB reinforced rubber composites on the tire magic triangle, Reprinted from Ref. [3].

As can be observed in Fig. 8, the partial replacement of CB with sustainable bio-fillers decreases the rolling resistance concerning CB-reinforced rubber composites. Such results could be attributed to the interruption of the CB network by adding a secondary filler, which will form and reform as an external force is applied (Payne effect). Furthermore, since bio-fillers are typically hydrophilic, they interact better with water which causes wet traction improvement. On the other hand, in bio-fillers' presence, the wear resistance could be reduced as these fillers are soft compared to CB or silica [3].

Numerous studies have focused on incorporating biofiller into rubber composites, exploring their potential as sustainable alternatives. In the following sections, the features of various biofillers and their impact on rubber composites' properties are discussed in detail.

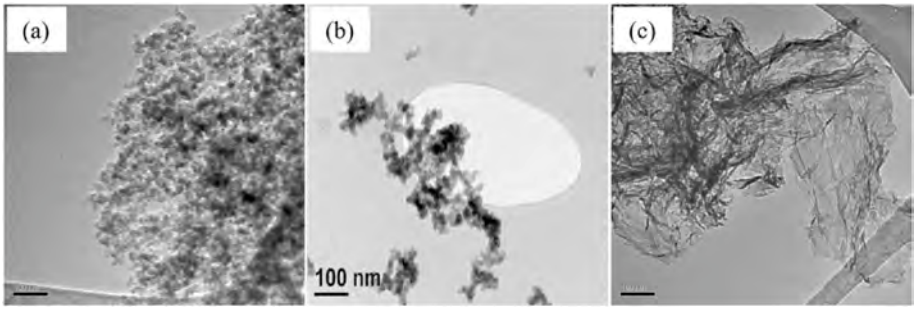

Fig. 9. TEM images of (a) commercial-grade silica (Zeosil 1165) and recovered silica fillers (b) rSilica; (c) geoSilica, Reprinted from Ref. [92].

4. Bio-fillers for rubber composites sustainability

4.1. Green silica

Nowadays, countless efforts have been made to use plant materials to produce green silica as an eco-friendly technique. The benefits of this trend are their abundance, low cost, deletion of chemical substances, and reduced energy consumption [82]. Various agricultural wastes are used to synthesize green silica, such as bamboo culm, sugarcane bagasse ash, rice husk ash, oil palm ash, wheat straw, corn stalks, Cassava periderm, and corncob ash [83–88]. Among them, rice husk ash (RHA), sugarcane bagasse and bamboo leaf contain a high silica content of up to 85–95%, 92.5%, and 61%, respectively.

Green silica has a potential reinforcement in rubber composites. It offers several benefits in terms of high modulus, tear strength, heat resistance, abrasion resistance, hardness, reduction in heat build-up, and rupture resistance. In other words, the presence of the silanol functional group on the surface of green silica improves hardness, modulus, abrasion resistance, and rheological features. In contrast, it reduces the beginning time of vulcanization [89].

Huabcharoen et al. [90] studied the cure characteristics and mechanical features of NR compounds filled with silica (15 phr) obtained from bagasse ash (BA) as reinforcing filler. They treated the BA with various processes, including hydrochloric acid (HCl) and HCl-ammonium fluoride (HCl–NH_4F). The purification of BA by HCl and HCl–NH_4F increased the silica content to 90.6% and 97.0%, respectively, compared with untreated BA with 77.2% silica. Moreover, purifying the silica caused to longer cure time and lower cross-linking. Indeed, the purification processes acted as an obstacle to rubber-rubber cross-linking while helping to minimise the filler-filler interaction. BA-filled NR compounds' tensile strength and elongation (in the range of 900%–1100%) improved in the presence of HCl–NH_4F-treated silica. Ooi et al. [91] used oil palm ash (OPA) as a reinforcement filler in NR vulcanizate, and the obtained results were compared with two commercial fillers (i.e. silica and CB). It was revealed that the scorch time and cure time of CB-filled NR was the lowest with respect to OPA and silica-filled NR vulcanizates. Nevertheless, incorporating OPA into NR led to the highest cure rate index. In the reinforcement perspective, CB-filled NR exhibited the highest tensile strength of 26 MPa, followed by OPA and commercial silica, with 25 MPa and 23 MPa, respectively. It was noticeable that adding silica and CB diminished the elongation at the break of the NR compound, whereas, in the presence of OPA, it increased by 7.4%.

Recently, Zaeimoedin et al. [92] used two kinds of silica recovered from tyre pyrolysis (rSilica) and geothermal water sources (geoSilica) as reinforcing fillers in ENR compounds to improve the sustainability of green tire tread compounds. The physical and mechanical properties of the rSilica/ENR and geoSilica/ENR composites were compared with the commercial-grade silica (Zeosil 1165). The results showed that rSilica/ENR composite had good physical features, including tensile strength, hardness and abrasion resistance, and good processing properties concerning Zeosil, which attributed to the ultimate particle diameter of rSilica (about 20 nm). Based on the TEM images (Fig. 9b), it can be supposed that the pyrolysis process had no noticeable impact on the rSilica ultimate particle size. Silica filler with a small particle size has a high specific surface area that can affect the filler's reinforcing effect [93]. Moreover, modified rSilica-ENR compounds with X50S silane coupling agent presented better physical characteristics than the non-silane compound, indicating that rSilica still can react with the silane. However, the pyrolysis process reduced the number of silanol groups on the silica surface. In the case of geoSilica, it was in the thin film form (Fig. 9c) without small spherical particles, which can influence the mixing process and the composite reinforcement.

Rice is one of the most important foods worldwide, generating about 22 wt% husks during milling. The produced husk is largely utilized as boiler fuel for energy production, creating a large amount of rice husk

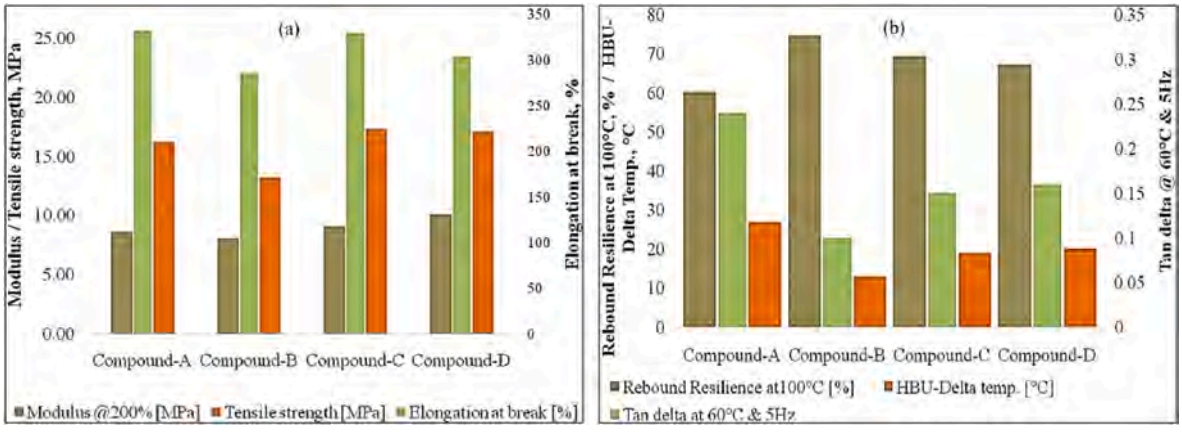

Fig. 10. CB/RHS/(SSBR-BR) rubber composites, (a) physico-mechanical properties; (b) dynamic mechanical characteristics, Reprinted from Ref. [97].

ash (RHA). Among agricultural waste materials, RHA contains the highest silica content, ~90% in amorphous form, making it an available source and cheap alternative for silica production [94].

Since disposing of waste rice husk is challenging and poses an important environmental issue [95], extensive research has been conducted to utilize this material and its ash as reinforcement in rubber composites. For example, Lolage et al. [96] studied the effect of replacing CB with RHA and two various commercial silica (Zeosil 200 MP and Ultrasil VN3) in a typical tire tread rubber formulation. They found that the composites with RHA had better reinforcement factors such as modulus at 100% and 300% (M300/M100), highest tensile strength and elongation at break as well as greater dispersibility in the tire rubber matrix (SBR/BR) with a potential of reduced rolling resistance than both the commercial references. Recently, Parmar et al. [97] investigated the physico-mechanical and dynamic mechanical properties of solution SBR (SSBR)/BR composites by partial and complete replacement of CB with precipitated rice husk silica (RHS). They prepared four different composites, including 100% CB (Compound-A), 100% RHS (Compound-B), 50% CB-50% RHS (Compound-C), and a higher amount of total filler (more RHS than CB, Compound-D). Compared to Compound A, rebound resilience at 100 °C and abrasion resistance index increased in Compound C, whereas heat buildup, dynamic modulus and tan delta decreased (Fig. 10). Increasing the total filler content in a rubber compound (Compound-D) showed an improvement in the dynamic modulus, heat build-up, rolling resistance, and abrasion loss with a lower elongation at break compared to Compound A. Such a finding could be due to the increase of reinforcement effect and restricting the rubber chains' movement. However, by 100% replacing CB with RHS (Compound B), there were no comparable physical and dynamic characteristics, specifically tensile strength, and complex modulus.

Choophun et al. [98] evaluated the loading effect of modified rice husk (Si69-RHS) on the mechanical properties of natural rubber composites. The experimental results showed that rising silica loading from 10 to 50 phr increased the scorch and cure times, hardness, and modulus. At the same time, there was a slight reduction in elongation at break and abrasion resistance. The tensile strength of Si69-RHS/NR composites reached the maximum value at 20 phr and then decreased by higher filler loading due to the silica agglomeration in the rubber matrix. Moreover, higher silica loading inhibited the movement of rubber chains due to the strong interaction between filler and the rubber matrix resulting in stiffer and harder-filled composites. Shiva et al. [99] extracted amorphous and pure silica from rice husks using thermal and sol-gel methods. They studied the effects of the extracted silica loading in two standard adhesion systems in the tire formulations, namely, rubber adhesion to resorcinol-formaldehyde-latex (RFL) coated polyester cords and rubber adhesion to brass-plated steel cords. Obtained results showed that the pH of the precipitation has a noticeable effect on the behaviour of rubber cord adhesion by controlling the silica surface area. They reported the decarbonization temperature of 700 ± 100 °C and the pH of 6 as favourable operating conditions for synthesizing amorphous silica, particularly for applications related to rubber-to-cord adhesion systems. Chundawat et al. [100] partially replaced CB with conventional precipitated silica and RHS (15, 30, and 50 phr) in a basic tread formulation. The results revealed that the properties of rubber compounds with RHS were comparable with those of conventional silica. Partial replacement of CB with conventional silica and RHS caused a slower cure rate, higher rebound resilience, lower heat generation, abrasion loss and tan delta, whereas had no remarkable change in physical characteristics. Based on obtained results, they suggested RHS as a sustainable alternative filler in tire formulation. Moreover, partially replacing CB with RHS improved the heat build-up, rolling resistance, and abrasion loss. Qian et al. [101] conducted a study on a pyrolytic RHA-filled NR/BR composite to explore how filler size and polymer crosslinking degree affect the Mullins effect. The results indicated that increasing the crosslinking degree of the NR/BR matrix reduced

Table 3
Mechanical properties of green silica-reinforced rubber composites.

Rubber composites	Filler loading	Mechanical characteristics	Source of silica/ Modifier	Ref
Nano-Silica/NR	Unfilled NR (control)	- Tensile strength (MPa): 19.54 - Elongation at break (%): 815.42	–	[102]
	Silica: 8 phr	- Tensile strength (MPa): 22.03 - Elongation at break (%): 880.86	Rice husk	
Silica/CB/ NR	Silica: 50 phr CB: 10 phr (control)	- Hardness (∘ Sh A): 72 - Abrasion loss (mm^3): 89 - Cross-link density (mol/ m^3): 1.344	Conventional silica	[100]
RHS/CB/NR	RHS: 50 phr CB: 10 phr	- Hardness (∘ Sh A): 72 - Abrasion loss (mm^3): 90 - Cross-link density (mol/ m^3): 1.286	Rice husk	
Silica/CB/ ENR	Silica: 55 phr CB: 3 phr	- Tensile strength (MPa): 22.7 - Modulus 100% (MPa): 2.4 - Hardness (IRHD): 65 - Elongation at break (%): 438 - Heat build-up (°C): 65.4 - DIN abrasion resistance (%): 95	Commercial-grade silica/X50S	[92]
		- Tensile strength (MPa): 22 - Modulus 100% (MPa): 2.3 - Hardness (IRHD): 64 - Elongation at break (%): 446 - Heat build-up (°C): 74.2 - DIN abrasion resistance (%): 67	Silica recovered from tyre pyrolysis/X50S	
Silica/NR	Silica: 20 phr	- Tensile strength (MPa): 20.9 ± 1.8 - Young modulus (MPa): 1.04 ± 0.11 - Hardness (∘ Sh A): 33.2 ± 0.8 - Elongation at break (%): 734 ± 35 - Abrasion loss (%): 0.06 ± 0.01	Rice husk waste/ Si69	[98]
Silica/NR	Silica: 12 phr	- Tensile strength (MPa): 17.98 - Tear strength (Kgf): 19.6 - Hardness (∘ Sh A): 60.8 - Elongation at break (%): 442.77	RHA/Unmodified	[89]

(*continued on next page*)

Table 3 (*continued*)

Rubber composites	Filler loading	Mechanical characteristics	Source of silica/ Modifier	Ref
		- Abrasion loss (% wt): 5.66		
Silica/CB/ NR	CB: 25 phr Silica: 5 phr	- Tensile strength (MPa): 23.74 - Modulus 300% (MPa): 7.65 - Tear strength (N/mm): 61.34	Rice husk derived RHNC/ Unmodified	[103]
	CB: 30 phr Silica: 0 (control)	- Tensile strength (MPa): 24.12 - Modulus 300% (MPa): 8.11 - Elongation at break (%): 554 - Tear strength (N/mm): 63.12		
Silica/CB/ NR	CB: 45 phr Silica: 5 phr	- Tensile strength (MPa): 13.769 ± 0.71 - Hardness (∘ Sh A): 43.4 - Elongation at break (%): 467 ± 44 - ARI: 56.23 ± 2.7 - Modulus 300% (MPa): 60.56 ± 0.34	Kerala rice husk nano ash/ Unmodified	[104]
Silica/NR	Silica: 1 phr	- Tensile strength (MPa): 25.2 - Elongation at break (%): 1126.5 - Modulus 300% (MPa): 1.661 - Hardness (∘ Sh A): 41	Oil palm ash (OPA)/ Unmodified	[105]

RHS: Rice husk silica; **RHA**: Rice husk ash; **CB**: Carbon black; **RHNC**: Rice husk derived type-I nanocellulose; **NR**: Natural rubber, **ENR**: Epoxidized natural rubber; **OPA**: Oil palm ash; **X50S**: Silane coupling agent; **Si69**: Triethoxysilyl tetrasulfide sulfur silane coupling agent Crosile-69; **DIN**: Deutsches Institute for Normung; **ARI**: Abrasion Resistance Index.

dissipation ratios with similar slop. These results were comparable with the increase of dissipation ratios as the filler size increased. These findings were further confirmed by a simulation on the composites with larger particle sizes of RHA, revealing higher strain energy density as strain levels increased from 25% to 35%. Furthermore, the dependence of the dissipation ratio on matrix crosslinking degree and the filler size is expected to reflect the Mullins effect, offering potential improvements in the engineering performance and durability of rubber products. The green silica-filled rubber composites and their mechanical properties are listed in Table 3.

4.2. Cellulose (nanocrystalline and microcrystalline cellulose)

Cellulose is the sustainable and the most abundant polysaccharide found on Earth, which derives from various natural sources such as plants, algae, fungi, and bacteria [106]. It is renewable, eco-friendly, biodegradable with excellent thermomechanical qualities, low density, low-cost, and non-toxic [107]. Cellulose and its derivatives, such as microcrystalline cellulose or cellulose microcrystals (MCC) [108], nanocrystalline cellulose (CNC), nano fibrillated cellulose [109], and cellulose esters [110] have attracted a lot of research interest as potential renewable reinforcing fillers in rubber composites. During the mixing of cellulose with rubber, cellulose tends to agglomerate within the matrix due to the presence of surface hydroxyl groups. Therefore, before mixing, surface modification treatments are often carried out on cellulose to facilitate its effective dispersion in the rubber matrix and ensure better integration and properties of the resulting composite material [111].

Among various types of cellulose, the investigation of the nanocrystalline has been on the increase owing to several desirable characteristics, such as high surface area, high aspect ratio, high crystallinity, high strength, high modulus, low density, mechanical flexibility, biodegradability and biocompatibility [112,113]. The distribution and interactions of CNCs within the rubber matrix substantially impact the mechanical properties of rubber composites. Recently, Jantachum et al. [114] examined the impact of silane coupling agent (3-triethoxysilylpropyl tetrasulfide (Si-69)) and CNCs loading (0–5 phr) on the properties of acrylonitrile butadiene rubber (NBR)/NR nanocomposites. The NBR/NR nanocomposites containing Si-69 showed improved interaction between CNCs and the rubber matrix, which caused the smoother continuous phase as illustrated in Fig. 11b–d and f. Moreover, compared to nanocomposites without silane, these composites showed increased thermal aging and mechanical characteristics such as hardness, abrasion resistance, tensile strength, and elongation at break (Fig. 11g, h, i and j). However, at higher CNCs loadings (greater than 1 phr), the mechanical properties of nanocomposite without silane deteriorated because of the phase separation, filler agglomeration, and the formation of cracks on the nanocomposite surfaces (Fig. 11c and e). Such results could be due to an inhomogeneous distribution of CNCs in the NBR/NR matrix at higher loadings (3 and 5 phr) and poor interfacial interaction between the CNCs and the polymer matrix, leading to reduced abrasion resistance, tensile strength, and elongation at break.

Jiang et al. [115] modified CNC isolated from softwood pulp by cetyltrimethylammonium bromide (CTMAB) to reinforce NR. They proposed that in the presence of 5 or 10 phr modified-CNC (m-CNC), the tensile strength, elongation at break and tear strength of m-CNC/NR composites were enhanced by 133%, 20%, and 66%, respectively, concerning pristine NR composites. Furthermore, wet-skid resistance and ageing resistance of NR composites significantly improved. In another study [116], CNC was modified with the cation surfactant cetyltrimethylammonium bromide and used as a partial replacement for CB in NR composites. The study's findings demonstrated a significant increase in tensile strength, elongation at break, tear strength, and wear resistance of the composites. These improvements can be attributed to CNC's surface modification, which improved CNC's dispersion in the matrix and developed interfacial interaction between filler and NR. Rashid et al. [117] used CNC as a reinforcement agent to increase the heat resistance and thermal stability of NBR composites. Adding 2 phr CNC remarkably improved the storage modulus (by 12 GPa), thermal stability and activation energy (up to 75%) of the CNC/NBR composites due to the good interfacial bonds between CNC and NBR, hydrogen bond formation, crystalline nature, and CNC's nanosized structure. Zhu et al. [118] prepared CNC/GO/NR nanocomposites. The self-assembled nanohybrids of CNC and GO showed a preferential dispersion within the interstitial spaces between latex microspheres, which formed a three-dimensional (3D) hierarchical conductive network. This unique arrangement and strong hydrogen bonding interactions between CNC and GO significantly enhanced electrical conductivity and mechanical properties, specifically tensile strength, and modulus. Compared to nanocomposites containing only 4 wt% GO, the nanocomposite with 4 wt% GO and 5 wt% CNC exhibited a remarkable nine-order of magnitude increase in electrical conductivity. Additionally, the electrical percolation threshold of the nanocomposite was three times lower than that of GO/NR composites, indicating a superior conductive behaviour. Table 4 summarises some of the significant mechanical characteristics of cellulose-reinforced rubber composites.

4.3. Lignin

Lignin (LGN) is a highly aromatic natural polymer with a three-dimensional amorphous structure. It is known as the second most available renewable natural polymer after cellulose which finds in all

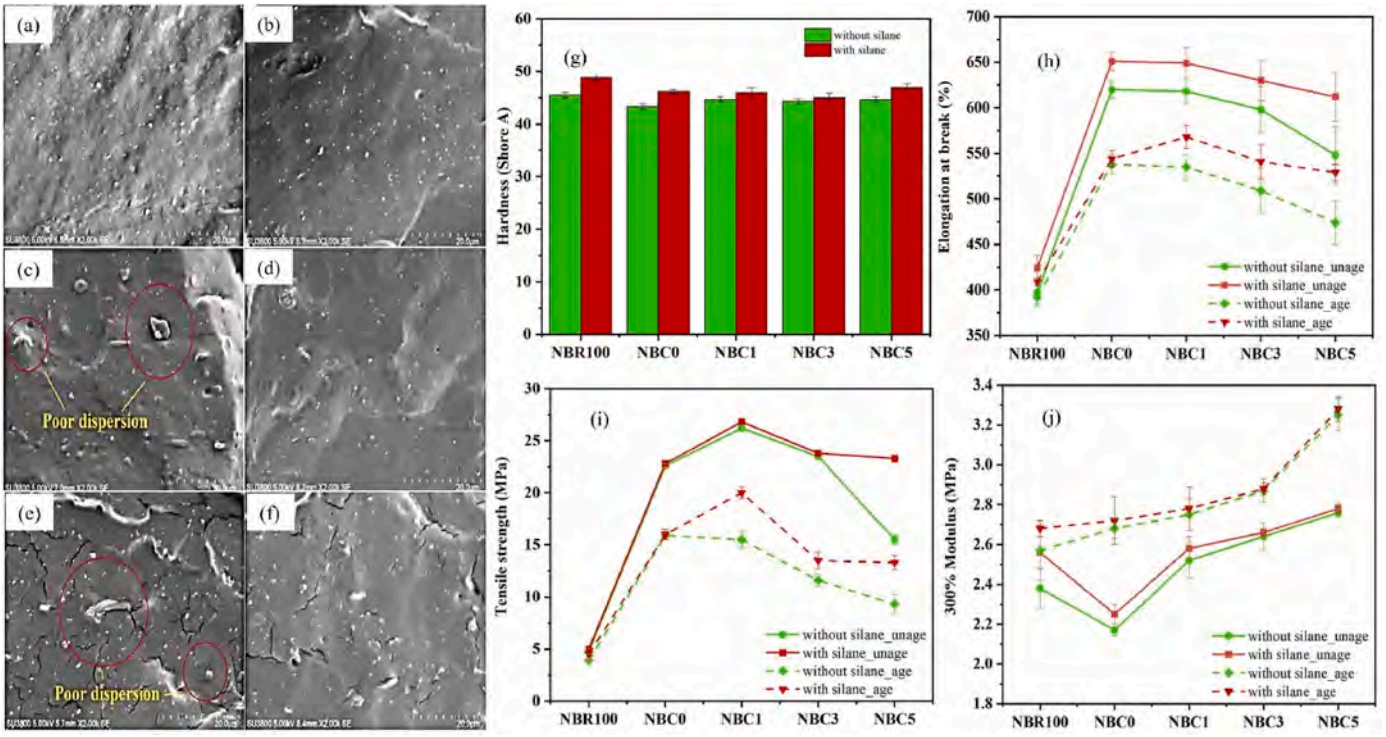

Fig. 11. SEM micrographs (× 2000 magnitude) and mechanical properties of NBR/NR nanocomposites containing various CNCs loadings with and without silane agent, (a) 1 phr CNC; (b) 1 phr CNC–Si69; (c) 3 phr CNC; (d) 3 phr CNC–Si69; (e) 5 phr CNC; (f) 5 phr CNC–Si69, (g) hardness (Shore A); (h) elongation at break; (i) tensile strength; (j) modulus at 300%, Reprinted from Ref. [114].

kinds of lignocellulosic materials, specifically in woods (~15–25 wt%). Based on the source, LGN organizes into three categories: softwood lignin, hardwood lignin and grass lignin [126,127]. LGN possesses various beneficial properties, such as good stability, low density, reinforcing effect, biodegradability, antioxidant, adhesive feature, high availability, low cost, renewability and mechanical reinforcement capacity [128,129]. These characteristics can be affected by LGN origin and applied extraction techniques. Table 5 shows different extraction techniques of LGN and the properties of obtained lignin [130].

Although LGN is mainly produced as a waste by-product from paper and pulp mill industries, only 2% have been successfully utilized for industrial purposes [131]. LGN has been successfully incorporated into rubber matrix for multiple purposes, including mechanical reinforcement, enhancement of adhesive properties, improvement of thermal oxidation stability of rubber, and as filler [132,133]. There are three different mixing methods to prepare LGN-rubber composites: mechanical mixing, latex mixing, and soft processing. The function of LGN-reinforced rubber composites is influenced by ash content, the LGN average molecular weight and distribution, LGN concentration in the matrix, purity, processing methods, and LGN compatibility with the rubber matrix [133].

For the first time, in the early 2000s, Setua et al. [134] used LGN as a reinforcing filler in NBR composites. Since then, only a few research articles have been published on LGN-based green rubber technology advancements. However, in the last decade, a considerable body of literature has grown up around the application of LGN as a reinforcing agent for developing bio-based sustainable rubber composites, especially in NR, SBR, acrylonitrile-butadiene rubber (ANBR), and polyethene-co-vinyl acetate (EVA) [135,136]. Furthermore, LGN has gained increased consideration as an alternative to CB in rubber composites for the tire industry and automotive devices [130]. Table 6 presents the main mechanical features of rubber composites containing various kinds of LGN.

Recently, Aini et al. [137] assessed the impact of a hybrid CB/LGN system on the properties of NR/BR composites. They incorporated three types of LGN (KL, OL, and SL) into the rubber matrix at filler loadings ranging from 5 to 20 phr while keeping the total filler content fixed at 50 phr. Compared to the SL-reinforced NR/BR composite, the composites filled with KL and OL had superior properties like processability, thermal stability and resistance to ageing. Besides, as can be observed in Fig. 12e, the incorporation of LGN in the NR/BR matrix reduced the Payne effect concerning composite without lignin as the control sample (NR/BR/CB 50phr). By adding 10 ph kL into the rubber matrix, the resulting composite exhibited comparable features to the control sample, possibly due to increased filler-filler interactions from the abundant hydroxyl groups on the LGN surface. The improved filler-filler interactions, however, led to poor filler dispersion in the rubber matrix, as the filler tended to agglomerate and interfere with cross-linking during vulcanization. The SEM micrograph confirmed these results, which showed agglomerated filler particles (Fig. 12(b–d)).

In another study, Aini et al. [138] evaluated the impact of two different types of compatibilizers, namely epoxidized NR with 50 mol% of epoxide group (ENR-50) and liquid butadiene rubber (LBR-352), on CB/LGN-filled NR/BR composites. The findings revealed that incorporating 10 phr ENR in the rubber composites improved the dispersion of the filler and enhanced interaction between composite and ENR. As a result, the composites' mechanical, flexibility, and dynamical properties were enhanced. Although the composites with LBR exhibited the weakest filler-filler interaction, they improved the rubber composites' processability and flexibility. Yu et al. [136] explored the incorporation of LGN in NR composites as a partial replacement for silica (30silica/20lignin). They reported that adding LGN in the NR composite reduced the Payne effect and improved the processability, anti-ageing resistance, and resistance against flex cracking of the composites. Furthermore, the composite exhibited high wet grip properties and low rolling resistance, desirable for tire applications. Hait et al. [139] used waste LGN as a BR reinforcing filler. They compared its mechanical properties with the same loading of standard fillers such as commercial

Table 4
Mechanical properties of cellulose-reinforced rubber composites.

Rubber composites	Filler loading	Mechanical characteristics	CNC Source/Modifier	Ref
Hybris (MCC–SiO_2)/SSBR/silica composite	Silica: 50 phr MCC–SiO_2: 0 (control)	- Tensile strength (MPa): 13.9 - Modulus at 200 % (MPa): 8.07 - Tear strength (kN/m): 41.3 - Hardness (∘ Sh A): 74.0	–	[119]
	Silica: 40 phr MCC–SiO_2: 10 phr	- Tensile strength (MPa): 13.5 - Modulus at 200 % (MPa): 7.54 - Tear strength (kN/m): 41.2 - Hardness (∘ Sh A): 71.0	Hybridized with nano-SiO_2	
Cellulose/NR	Unfilled NR (control)	- Tensile strength (MPa): 0.63 - Young's modulus (MPa): 0.69	–	[120]
	Cellulose: 30 phr	- Tensile strength (MPa): 6.03 - Young's modulus (MPa): 20.08	In Situ RC from alkaline urea- aqueous system	
CNC/NR	CNC: 10 phr	- Tensile strength (MPa): 30.3 - Elongation at break (%): 670.4 - Tear strength (kN/m): 40.3	Softwood pulp/CTMAB	[115]
CNC–RGO hybrid/NR	CNC–RGO hybrid: 2.08 vol%	- Tensile strength (MPa): 1.9 - Modulus (MPa): Improved	CNC-mediated assembly of graphene	[121]
TCNCs/CSBR	Unfilled CSBR (control)	- Tensile strength (MPa): 3.58 ± 0.15 - Elongation at break (%): 524 ± 22 - Modulus at 100% (MPa):0.95 ± 0.05 - Toughness (KJ/m^2): 1025 ± 48	–	[122]
	TCNCs: 15 phr	- Tensile strength (MPa): 14.11 ± 0.41 - Elongation at break (%): 226 ± 20 - Modulus at 100% (MPa):8.96 ± 0.35 - Toughness (KJ/m^2): 2091 ± 78	Softwood pulp/Epoxy-functionalization modification of the TCNCs	
CNC/Unoxidized NR	Unfilled NR (control)	- Modulus (MPa): 1.33 ± 0.39 - Strain at break (%): 878 ± 57 - Strength (MPa): 1.72 ± 0.39	–	[123]
CNC/Oxidized NR	CNC: 5 wt%	- Modulus (MPa): 0.72 ± 0.03 - Strain at break (%): 202 ± 58 - Strength (MPa): 0.11 ± 0.02	Oxidized NR using $KMnO_4$ as oxidant	
CNC/NR	Unfilled NR (control)	- Tensile strength (MPa): 3.52 - Elongation at break (%): 860 - Modulus at 200% (MPa):2.05	Jute fibres	[124]
	CNC: 3 wt%	- Tensile strength (MPa): 4.25 - Elongation at break (%): 410 - Modulus at 200% (MPa):3.40		
CNC/NR	Unfilled NR (control)	- Tensile strength (MPa): 3.59 ± 1.00 - Modulus at 100% (MPa): 0.64 ± 0.02	–	[125]
	CNC: 5 phr	- Tensile strength (MPa): 4.32 ± 0.76 - Modulus at 100% (MPa): 0.67 ± 0.01	Ramie fibre	
		- Tensile strength (MPa): 10.46 ± 0.94 - Modulus at 100% (MPa): 1.02 ± 0.09	Ramie fibre/APTES	
		- Tensile strength (MPa): 9.5 ± 1.63 - Modulus at 100% (MPa): 1.03 ± 0.02	Ramie fibre/TESPT	
		- Tensile strength (MPa): 10.76 ± 1.92 - Modulus at 100% (MPa): 1.25 ± 0.03	Ramie fibre/MPTMS	

MCC: Microcrystalline cellulose; **CNC**: Cellulose nanocrystalline; **TCNCs**: Tunicate cellulose nanocrystals; **NR**: Natural rubber; **SSBR**: Solution-polymerized styrene-butadiene rubber; **CSBR**: Carboxylated styrene-butadiene rubber; **RC**: Regenerated cellulose; **CTMAB**: Cetyl trimethyl ammonium bromide; **CB**: Carbon black; **RGO**: Reduced graphene oxide; APTES: 3-aminopropyltriethoxysilane; **MPTMS**:(3-mercaptopropyl) trimethoxysilane; **TESPT**: bis-(3 triethoxysilylpropyl) tetrasulfide.

silica and CB. It found that the values of tensile strength (TS) and elongation at break (EB) of LGN (50phr)-BR composites increased to ~10 MPa and ~276%, respectively, compared with the BR composites containing CB (~8.5 TS, ~224% EB) and a silica-silane system (~7.34 TS, ~229% EB). Khan et al. [140] fabricated SBR composites containing nanographene oxide and LGN (1–3 wt%) for automobile tyre application. The microscopy examination showed that adding GO improved the morphology of pure SBR composite to a compact structure with a smoother surface (Fig. 13a and b). Incorporating 1 wt% LGN into the GO/SBR composite exhibited well-integrated morphology (Fig. 13c) containing crest-and-trough-like features, which confirmed the strength of molecular interaction between GO and SBR rubber. These composites

Table 5
Various extraction methods of LGN and related characteristics.

Extraction methods of lignin			
Sulfur bearing process		Sulfur-free process	
Kraft lignin (KL)	Sulfite pulping (Lignosulfonate, LS)	Alkaline pulping (Soda lignin, SL)	Solvent pulping (Organosolv lignin, OL)
- Ash content of 1–2%	- High ash content of 4–8%	- Higher purity than KL and LS	- High reactive groups and high purity
- Molecular weight of 3,000–188,000 g/mol	- High molecular weight than KL 1,000 to 50,000 g/mol	- Contains lower phenolic and aliphatic hydroxyl groups	- High-quality lignin for higher value-added applications
- Used as dispersing agents, additives, thermoset polymers, thermoplastic mixtures and copolymer	- Required to modify	- Suitable for a range of high products (resins, chemical reactants, composites, and antioxidant agents)	- High solubility in an organic solvent but insoluble in water
- Low-value-added applications	- Exceptional colloidal properties, dispersants, additives (plasticizers), surfactants, and flocculants		

had better tensile strength and elongation at break than other composites (with 2 and 3 wt% LGN) due to the excellent interface and adherence between bio-fillers imparting a good stress transfer feature (Fig. 13e). Besides these, this composite possessed the best elasticity and stiffness. Meanwhile, improving porosity in SBR/GO/1.0LGN composite with excellent surface area imparts it to use as a green tire in automobile industrial fields. On the contrary, incorporating 2 wt% LGN formed large protuberances (Fig. 13d), owning to the aggregation effect of LGN fibrils, which remarkably formed in the 3 wt% LGN filled SBR composite.

Intapun et al. [141] investigated the potential application of Klason LGN (from rubberwood) as an alternative reinforcing filler for high-performance, eco-friendly NR biocomposites. With the incorporation of LGN up to 15 phr, its reinforcement effect enhanced stress while it declined in the presence of 20 phr filler. Such a finding could be due to the reinforcement mechanism of LGN through strain-induced crystallization. Moreover, NR composites containing 10 phr filler had the highest mechanical properties in terms of stress-strain, 100% modulus, and tensile strength owning to interactions between the Klason LGN filler and NR matrix. Hosseinmardi et al. [142] investigated the effects of the addition of nanoscale organosolv lignin (OL) particles (1, 2, 5, 10, and 20 wt%) on the properties of NR latex. The NR composites containing 5 wt% OL exhibited the best results with increased tensile strength, toughness, and Shore A hardness by 39%, 53%, and 12%, respectively, whereas they retained high elongation at break (~1800 %).

4.4. Starch (St)

Starch (St) is a polysaccharide with a rigid structure and crystalline content that can be derived from various sources, such as cereals (wheat, corn, rice), roots or tubers (potatoes and cassava), sugar, fruits, and vegetables [148]. It offers beneficial properties such as low density, environmental friendliness, abundance, renewable, and low cost, making it a promising reinforcing biofiller for rubber composites [149,150]. Several techniques to incorporate St in rubber composites include

Table 6
Mechanical properties of lignin-filled rubber composites.

Rubber composites	Filler loading	Mechanical characteristics	Processing method	Ref
Industrial sulfate lignin/SBR	Lignin: 50 phr	- Modulus at 300 % (MPa): 3.6 - Tensile strength (MPa): 16.4 - Elongation at break (%): 787.4 - Tear strength (kN/m): 49.4 - Hardness (∘ Sh A): 64.0	Co-coagulated by SBR latex and aqueous lignin solution	[143]
Industrial sulfate lignin/F51/ SBR	Lignin: 50 phr F51: 20 phr	- Modulus at 300 % (MPa): 10 - Tensile strength (MPa): 17.6 - Elongation at break (%): 539.7 - Tear strength (kN/m): 62.2 - Hardness (∘ Sh A): 76.0	Melt compounding method	
(OL)/NR	Unfilled NR (control)	- Modulus at 700 % (MPa): 3.1 ± 0.1 - Tensile strength (MPa): 28.3 ± 2.3 - Toughness (MJm-3): 131 ± 9 - Hardness after curing: 6.0 ± 0.8		[142]
	OL: 5 wt%	- Modulus at 700 % (MPa): 5.3 ± 0.1 - Tensile strength (MPa): 39.3 ± 1.7 - Toughness (MJm-3): 202 ± 16 - Hardness after curing: 61.0 ± 0.6		
Lignin/ENR	Lignin: 40 phr	- Tensile strength: decreased by 58% (compared to pristine ENR) - Tear strength: decreased by 32% (compared to pristine ENR) - Elongation at break: decreased by 21% (compared to pristine ENR)	Directly mixed rubber composites	[144]
		- Tensile strength: raised by 114% (compared to directly mixed NR) - Tear strength: raised by 23% (compared to directly mixed NR) - Modulus at 300 %: raised by 400% (compared to directly mixed NR)	High-temperature dynamic heat treatment (HTDHT)	
Lignin/SBR/ ENR	Unfilled SBR/ENR (control)	- Tensile strength (MPa): 2-3 - Tear strength: ~10 kN/m	–	[145]
	Lignin: 40 phr	- Tensile strength (MPa): 15-19 - Tear strength: 20–30 kN/m		

(continued on next page)

Table 6 (*continued*)

Rubber composites	Filler loading	Mechanical characteristics	Processing method	Ref
Softwood lignin/NR	Lignin: 5 phr	- Hardness (∘ Sh A): 45.5 ± 0.5 - Abrasiveness (cm^3): 0.0847 ± 0.0170 - Resilience (%): 57.6 ± 0.8	Glycerolysate plasticizer	[146]
Modified KL/ hydrophobic NR	Unfilled NR (control)	- Tensile strength (MPa): 23.6 - Elongation at break (%): 1017.7	Solvent casting technique	[147]
	KL: 5 wt%	- Tensile strength (MPa): 34		

NR: Natural rubber; **ENR**: Epoxidized natural rubber; **SBR**: Styrene-butadiene rubber; **BR**: Polybutadiene rubber; **F51**: Novolac epoxy resin; **OL**: Organosolv lignin, **KL**: Kraft lignin.

mechanical mixing, master batch blending, direct blending, coagulation, chemical modification, irradiation, grafting and blending. Adding St to the rubber matrix enhances its biobased content and mechanical properties. Moreover, it offers dual effects within the rubber system as both a reinforcing agent and a coupling agent, contributing to improved performance in rubber materials. Incorporating St in the rubber matrix, especially in tire application, improves its properties, such as wet grip increment, tire weight decrement, rolling resistance reduction, and reinforcing effect [151]. Nevertheless, rubber and St are incompatible due to their non-polarity and high polarity entities, respectively, which can impair the characteristics of St-rubber composites [152]. For this reason, three approaches have been proposed to improve the compatibility of St-filled rubber composites, including [153]:

- Modifying the polymer matrix before mixing it with St.
- Using a compatibilizer to enhance the interaction between St and the rubber matrix.
- Treating or modifying the St before mixing it with the polymer.

For example, Goodyear Tire Co [154]. utilized modified corn St in a finely dispersed state to improve the tire's characteristics. Wu et al. [155] esterified porous starch (PS) using dodecenyl succinate anhydride resulting in modified starch (MS) that exhibited reduced self-aggregation within the NR matrix. Compared with NR, incorporating 10 ph MS resulted in the highest cross-link density and improved the tensile strength, tear strength, and elongation at the break by 30%, 33% and 25%, respectively. Moreover, modified St increased the internal friction and caused a shift in the glass transition temperature to a lower value, thereby improving the rolling resistance of the composites. In another study, Du et al. [156] prepared modified porous starch PS/CB/NR composites. The experimental findings indicated that increasing the ratio of dodecenyl succinate anhydride-modified porous starch (DDSAPS) to CB led to a significant reduction in the Payne effect of rubber compounds, as well as a decrease in the mechanical properties of the vulcanized rubbers. These results can be explained by the potential aggregation of DDSAPS within the composite by increasing the ratio of DDSA-PS/CB. Additionally, incorporating DDSA-PS into the NR composites improved rolling resistance and reduced hysteresis, as evidenced by decreased heat build-up, making it an alternative filler to CB in the rubber industry. Sowińska-Baranowska et al. [157] used corn St as a biofiller in NR composites. To improve the dispersion of the biofiller in the NR matrix, they employed an ionic liquid (Bmicl) and aminosilane (3-aminopropyl)-triethoxysilane (APTES). The St/BmiCl/NR and St/APTES/NR composites exhibited enhanced cross-link density and improved mechanical properties in static and dynamic conditions compared to unfilled samples. In the unmodified St/NR vulcanizate (Fig. 14a), the solid particles were not homogeneously dispersed in the NR matrix and showed poor wetting by the elastomer matrix. In contrast, especially in 20 St/BmiCl vulcanizate (Fig. 14c), small aggregates of particles were homogeneously dispersed and well-wetted by the elastomer matrix, with no observed agglomeration. This improvement was attributed to the homogeneous dispersion of modified starch within the NR elastomer matrix and the resulting higher cross-link density, as confirmed by SEM analysis.

Uzoh et al. [158] partially replaced CB with Polynesian arrow root (PAR) St in NR through a new latex compounding procedure. This

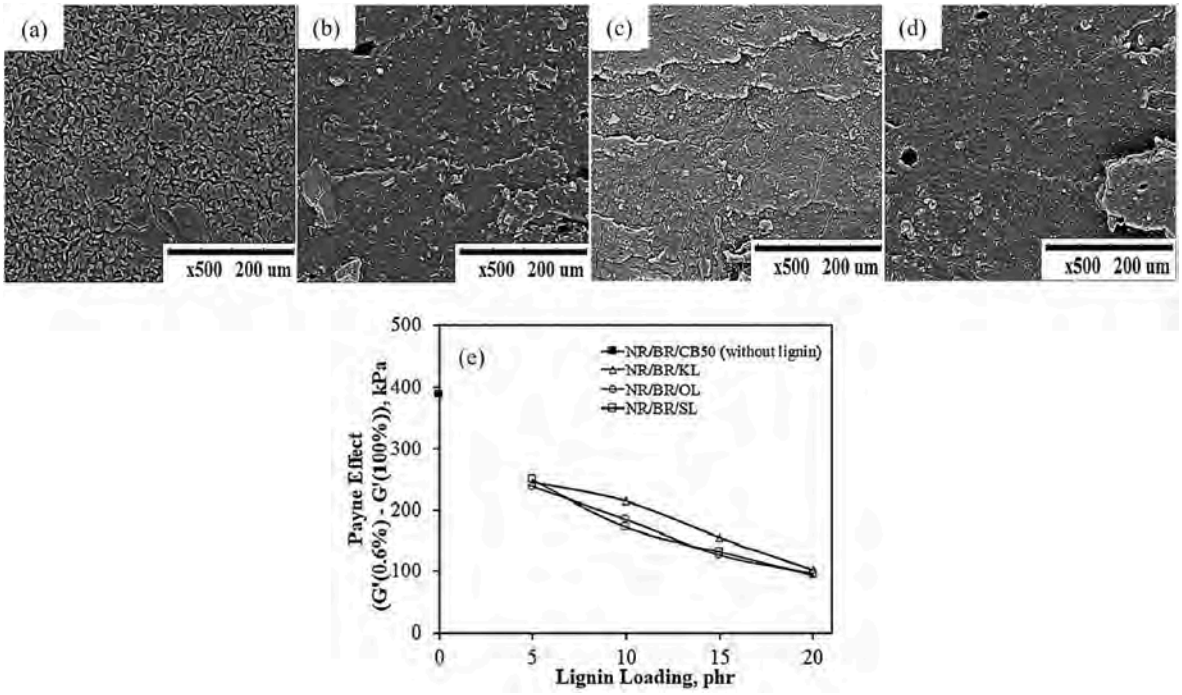

Fig. 12. FESEM image of NR/BR compounds containing (a) 50 phr of CB, (b) 10 phr of KL, (c) 10 phr of OL, (d) 10 phr of SL; (e) Payne effect of NR/BR compounds in the presence of different types of lignin, Reprinted from Ref. [137].

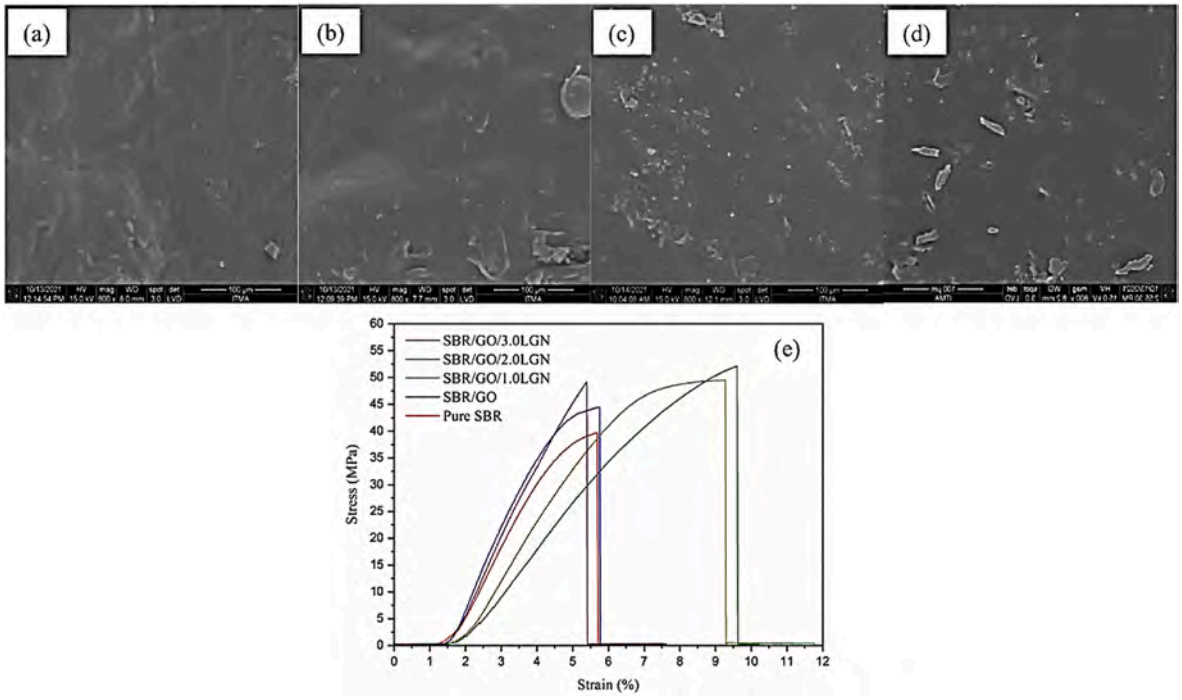

Fig. 13. FESEM image of (a) pure SBR, (b) SBR/GO, (c) 1.0LGN/GO/SBR, (d) 2.0LGN/GO/SBR under 800 × magnifications; (e) mechanical stress-strain curves of SBR/GO composites containing various lignin wt.%, Reprinted from Ref. [140].

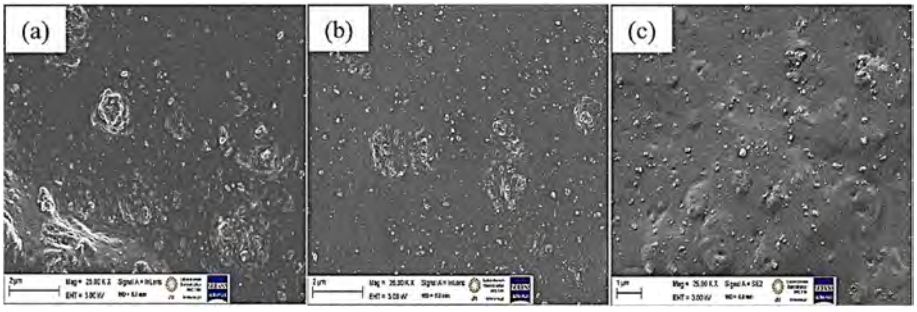

Fig. 14. SEM images of starch (20phr)-NR composites: (a) Unmodified St; (b) St/APTES; (c) St/BmiCl, Reprinted from Ref. [157].

method reduced the particle size of PAR St granules from a few micrometres to the nanoscale, allowing it to mix thoroughly with the NR molecules at a molecular level during the co-coagulation process and at compounding. The high values of cross-link density in the range of 20 phr–30 phr PAR St loading and the absence of phase separation during and after the compounding and curing processes showed strong filler-rubber interaction and adhesion at the interfaces. Moreover, PAR St as an alternative filler in NR provided moderately good reinforcement regarding physical and mechanical properties (tensile strength, resilience, and hardness) compared with unfilled NR and CB-filled NR composites. Based on the results, PAR St can replace CB and silica as fillers in NR in tire manufacturing with lower cost, weight, and energy consumption. Besides this, PAR St had the potential to completely substituted Cassava St and Maize St as a source of St filler in the rubber industry. Table 7 shows some reported mechanical properties of St/rubber composites.

4.5. Biomass-derived carbon (biochar)

Composite materials offer key features in terms of toughness, strength, weight reduction, chemical resistance, and corrosion resistance, which are important in diverse industries such as automotive, aerospace, sporting goods and electronic industries [163]. Carbonous reinforcements have a critical role in the strength and performance of composites. Among the carbon-based fillers, CB is widely used in rubber composites as a sustainable filler. However, due to environmental and global concerns, other fillers should partially or fully replace CB.

In recent years, a considerable body of literature has grown around bio-based carbon as a new, inexpensive, sustainable, and practical alternative carbonaceous filler for developing polymer and biocomposites. The thermochemical conversion of various types of biomasses in a limited oxygen environment (pyrolysis) at 400–600 °C resulted in a carbon-rich solid product known as biochar. Compared with CB, biochar lacks purity, while most industrial CB has more than 98% purity owing to its petroleum source. In the other word, biochar is produced from any carbon-containing biomass, so it contains different chemical compounds as a starting feedstock with less purity [164]. However, the pyrolysis conditions such as temperature, residence time and heating rate can control and optimize to manufacture biochar with tunable size, surface morphology, porosity, surface area, functional groups, intrinsic modulus, high carbon content (>90% carbon) and less ash content (<8%) [165,166]. In addition, bio-sourced carbon has variable surface chemistry that can be modified to achieve better compatibility between biofiller and rubbers. Table 8 compares the properties of

Table 7
Mechanical characteristics of starch-filled rubber composites.

Rubber composites	Filler loading	Mechanical characteristics	Processing method/ Modifier	Ref
PS/CB/NR	CB: 60 phr (control)	- Tensile strength (MPa): 26.9 - Tear strength (kN/m): 115.2 - Hardness (∘ Sh A): 77	Porous starch modified by esterification with (DDSA)	[156]
	PS: 20 phr CB: 40 phr	- Tensile strength (MPa): 20.1 - Tear strength (kN/m): 48.8 - Hardness (∘ Sh A): 75		
Starch/CB/ NR	CB: 60 phr (control)	- Tensile strength (MPa): 24.11 - Tear strength (kN/m): 79.83 - Hardness (∘ Sh A): 71	Starch nanocrystals prepared by acidolysis/ Unmodified	[159]
	PS: 25 phr CB: 35 phr	- Tensile strength (MPa): 21.43 - Tear strength (kN/m): 52.83 - Hardness (∘ Sh A): 64		
Starch/NR	Unfilled NR	- Tensile strength (MPa): 2.01	Electron beam irradiated method/starch modified with resorcinol–formaldehyde	[160]
Unmodified starch/NR	Starch: 5 phr	- Tensile strength (MPa): 3.82		
Modified starch/NR		- Tensile strength (MPa): 6.44		
Starch/CB/ SBR	Starch: 0 CB: 20 phr (control)	- Modulus at 300 % (MPa): 2.3 - Tensile strength (MPa): 9.5 - Elongation at break (%): 916 - Tear strength (kN/m): 40.0 - Hardness (∘ Sh A): 64.6	Emulsion polymerization	[161]
Starch/SBR	Starch: 20 phr	- Modulus at 300 % (MPa): 2.1 - Tensile strength (MPa): 3.3 - Elongation at break (%): 564 - Tear strength (kN/m): 21.3 - Hardness (∘ Sh A): 65.3	Emulsion polymerization/ Modified starch with methyl methacrylate	
		- Modulus at 300 % (MPa): 2.7 - Tensile strength (MPa): 9.7 - Elongation at break (%): 940 - Tear strength (kN/m): 43.7 - Hardness (∘ Sh A): 67		
Starch/NR	Unfilled NR (control)	- Modulus at 300 % (MPa): 1.2 ± 0.1 - Tensile strength (MPa): 10.4 ± 0.1 - Elongation at break (%): 820 ± 20 - Hardness (∘ Sh A): 31 ± 1	Unmodified	[157]
	Starch: 10 phr	- Modulus at 300 % (MPa):1.6 ± 0.1 - Tensile strength (MPa): 12.1 ± 0.2 - Elongation at break (%): 607 ± 22 - Hardness (∘ Sh A): 33 ± 1		
Starch/NR	Unfilled NR (control)	- Tensile strength (MPa): 21.9 - Elongation at break (%): 170.69 - Hardness (IRHD): 20-21	Latex compounding process/Unmodified	[158]
PAR Starch/ CB/NR	PAR: 0 CB: 30 phr	- Tensile strength (MPa): 87.6 - Elongation at break (%): 6807 - Hardness (IRHD): 66-88		
PAR Starch/ NR	PAR: 30 phr	- Tensile strength (MPa): 57.4 - Elongation at break (%): 10007 - Hardness (IRHD): 47-48		

(*continued on next page*)

Table 7 (*continued*)

Rubber composites	Filler loading	Mechanical characteristics	Processing method/ Modifier	Ref
Starch/CB/ SBR/BR	Starch: 0 CB: 10 phr	- Tensile strength (kg/cm^2): 144 - Elongation at break (%): 452 - Modulus at 300 % (kg/cm^2): 83.1	Unmodified	[162]
	Starch: 10 phr CB: 10 phr	- Tensile strength (kg/cm^2): 144 - Elongation at break (%): 433 - Modulus at 300 % (kg/cm^2): 91.6		

NR: Natural rubber; **SBR**: Styrene-butadiene rubber; **BR**: Butadiene rubber; **CB**: Carbon black; **DDSA**: Dodecenyl succinic anhydride; **PS**: Porous starch; **PAR**: Polynesian arrowroot.

Table 8
The comparison of CB and biochar.

Carbon filler	Feedstock	Preparation method	Carbon content	Structure
Biochar	Biomass (agro-waste, industrial by-products, and industrial co-products)	Pyrolysis of the biomass (at moderate to high temperatures)	40–90% (Greatly dependent on the pyrolysis conditions)	Amorphous carbon, microcrystals with abundant surface functional groups and porosity
Carbon black	Petroleum, coal tar, asphalt, etc.	Combustion of petroleum, coal tar, or asphalt under air-poor conditions	>95%	Microcrystal or amorphous carbon particles

biochar with conventional CB [167].

Since biochar is a renewable carbon source, it has gained more interest as an alternative filler to CB in rubber composites. Lay et al. [168] pyrolyzed dead leaf biomass at 1000 °C and used them as a promising and cost-effective alternative for CB filler in rubber composites. The dead leaf-activated carbon (DLAC) had high carbon purity of 82.6%. Incorporating 15 phr DLAC increased tensile strength and the modulus at 100% and 300% by 8% and 40%, respectively, while reducing the elongation at break and cross-link density by approximately 5% and 24%, respectively. Paleri et al. [169] studied the effect of various carbon-based fillers, including CB, biocarbon (BC), and a hybrid filler of both (BC-CB), on the properties of NR matrix. They produced BC by pyrolysis of dried distillers' grain with solubles (a co-product from the corn ethanol industry) at 900 °C. It was found that incorporating hybrid filler based on a sustainable CB and BC significantly reduced the rolling resistant features. Compared with CB, biocarbon's larger particle size negatively affects the rubber composites' tensile strength. Additionally, thermal characterization revealed similar transition and degradation mechanisms in all the filled NR composites, confirming a similar behaviour of BC and CB. Jiang et al. [170] converted waste LGN into nano-biochar (LB) and used it as a renewable replacement to CB for reinforcing SBR composite. The results showed that LB with a high specific surface area (83.41 m^2/g) had vesicle-like primary nano-particles, which formed "high-structure" irregular fragments. Incorporating 40 phr LB into the SBR matrix enhanced the tensile strength and elongation at the break to 7.1-folds and 2.4-folds, respectively. The difference in both fillers' surface characteristics and structural properties suggested distinct reinforcing mechanisms for LB and CB-filled rubber composites. Non-etheless, LB had a similar reinforcing effect on SBR compared to commercial CB (N330).

Recently, Lubura et al. [171] evaluated the effect of hydrothermally carbonized hardwood sawdust biomass (HC) as a reinforcing filler on the characteristics of the NR matrix. They used the combined filler containing CB and HC with various ratios, while the total content of the combined fillers was kept constant. In the presence of large amounts of HC, the cross-link density of composites reduced due to their larger particle size and smaller specific surface area. The NR composites with HC/CB ratios of 20/30 and 10/40 showed interesting chemical stabilization and good mechanical features. El-Aziz et al. [172] produced biochar from waste agriculture and used it in different ratios with CB as a reinforcement filer in the SBR composite. With the incorporation of 25%, 50%, 75%, and 100% biochar, the tensile strength of SBR decreased to 13.5 MPa, 11.2 MPa, 9.5 MPa, and 6.9 MPa, respectively, which were less than 100%CB/SBR composite (14.9 MPa). Moreover, by increasing the ageing time, the vulcanized sample containing 25% biochar exhibited higher retained tensile strength values concerning CB/SBR composite. Abidin et al. [173] studied the potential of Palm kernel shell (PKS) derived from palm oil waste as a sustainable and reinforcement biofiller in carboxylated nitrile butadiene rubber (XNBR) composites. The PKS hybridized with commercial CB (N660) in various loading ratios. By increasing the loading ratio of PKS in hybrid CB/PKS,

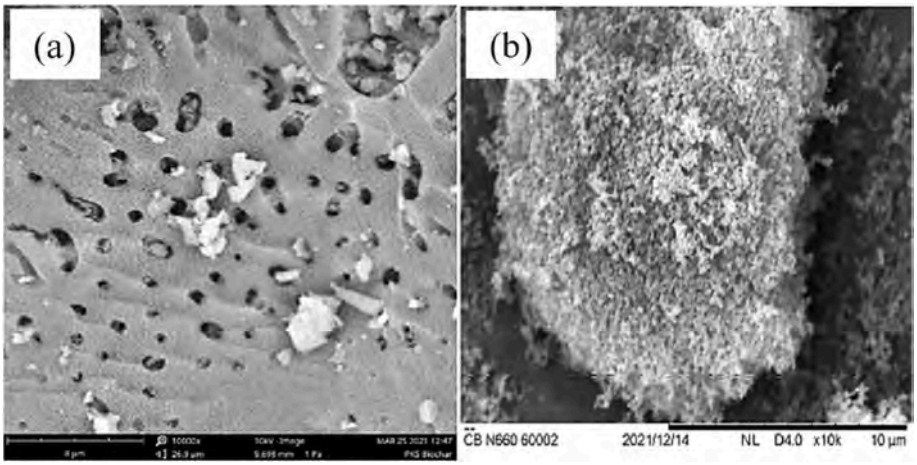

Fig. 15. SEM images of (a) PKS and (b) CB at × 10,000 magnification, Reprinted from Ref. [173].

Table 9
The mechanical characteristics of biochar-filled rubber composites.

Rubber composites	Filler loading	Mechanical characteristics	Source of biochar	Ref
CB/Biochar/PBR/NR	CB: 35 phr Biochar: 15 phr	- Tensile strength (MPa): 20.1 ± 1.1 - Elongation at break (%): 443 ± 6 - Toughness (MPa): 38.9 ± 3.0 - Young's Modulus (MPa): 4.3 ± 0.5	Coppiced hardwoods (Paulownia elongate) PAUL	[176]
	Biochar: 50 phr	- Tensile strength (MPa): 7.4 ± 0.4 - Elongation at break (%): 275 ± 39 - Toughness (MPa): 13.8 ± 2.9 - Young's Modulus (MPa): 7.6 ± 0.4		
	CB: 35 phr Biochar: 15 phr	- Tensile strength (MPa): 20.9 ± 1.2 - Elongation at break (%): 432 ± 21 - Toughness (MPa): 39.8 ± 4.1 - Young's Modulus (MPa): 4.2 ± 0.2	Coppiced hardwoods (Populus tremuloides) POP	
	Biochar: 50 phr	- Tensile strength (MPa): 7.0 ± 0.4 - Elongation at break (%): 307 ± 33 - Toughness (MPa): 14.0 ± 2.4 - Young's Modulus (MPa): 6.6 ± 0.7		
Biochar/NR	Biochar: 30 phr	- Tensile strength (MPa): 15.6 ± 2 - Elongation at break (%): 770 ± 70 - Tear strength (N/mm): 49 ± 5 - Modulus at 300% (MPa): 3.2 ± 0.29	DDGS (a co-product of the corn ethanol industry)	[169]
(CB-Biochar) hybrid/NR	Hybrid filler: 30 phr	- Tensile strength (MPa): 21.4 ± 2 - Elongation at break (%): 750 ± 73 - Tear strength (N/mm): 51 ± 5 - Modulus at 300% (MPa): 4.0 ± 0.38		
HTS-Coated biochar/SBR	HTS: 5 wt%	- Tensile strength (MPa): 11.4 ± 1.0 - Elongation at break (%): 683 ± 61 - Fracture toughness (MPa): 40.7 ± 6.8	Dry hardwood	[177]
PB/CB/NR	CB: 50 wt% PB: 50 wt%	- Tensile strength (MPa): 24.3 ± 0.4 - Elongation at break (%): 527 ± 12 - Toughness (MPa): 52.3 ± 1.4 - Young's Modulus (MPa): 2.8 ± 0.3	Silica (1%)-milled Paulownia elongate	[175]
Biochar/CB/SBR	CB: 50 wt% Biochar: 50 wt%	- Tensile strength (MPa): 6.86 ± 0.96 - Elongation at break (%): 518 ± 87 - Toughness (MPa): 16.92 ± 4.36	Birchwood	[178]
Biochar/SBR	Biochar: 100 %	- Tensile strength (MPa): 4.67 ± 0.26 - Elongation at break (%): 437 ± 44 - Toughness (MPa): 10.06 ± 1.33		
Biochar/NBR latex	Biochar: 40 phr	- Tensile strength (MPa): 6.67 - Elongation at break (%): 716 - Modulus at 300% (MPa): 3.29 - Hardness (∘ Sh A): 61.8 - Tear strength (N/mm): 32.4	Rice bran carbon	[179]
Biochar/SBR	Biochar: 60 phr	- Tensile strength (MPa): 3.7 ± 0.07 - Elongation at break (%): 461 ± 8 - CRI (min^{-1}): 4.58	Bamboo charcoal powder	[180]
Corn starch/Biochar/SBR	3:1 blend of corn starch: biochar	- Tensile strength (MPa): 1.74 ± 0.03 - Elongation at break (%): 769 ± 25 - Toughness (MPa): 7.5 ± 0.2	Corn stover feedstock	[181]
(HC-CB)/NR	CB: 30 phr HC: 20 phr	- Tensile strength (MPa): 7.52 - Elongation at break (%): 389 - Toughness (MJ/m^3): 10.4 - Hardness (shore A): 48.7	Carbonized hardwood sawdust waste	[171]
	CB: 40 phr HC: 10 phr	- Tensile strength (MPa): 8.52		

(*continued on next page*)

Table 9 (*continued*)

Rubber composites	Filler loading	Mechanical characteristics	Source of biochar	Ref
		- Elongation at break (%): 368 - Toughness (MJ/m^3): 11.7 - Hardness (shore A): 52.7		

PBR: Polybutadiene; **NR**: Natural rubber; **SBR**: Styrene–butadiene rubber; **NBR**: Nitrile rubber; **CB**: Carbon black; **DDGS**: Dried distillers' grains with soluble; **HTS**: Heat-treated starch; **PB**: Silica-milled Paulownia elongate; **HC**: Co-fillers 'hydrochar'; **CRI**: Cure rate index.

the cure time and cure rate index decreased and increased, respectively. Furthermore, the impact of PKS was comparable with CB since, by the high loading of PKS, the physicomechanical properties (abrasion resistance and hardness values) of XNBR composites increased due to the porous structure of PKS (Fig. 15a). The porous structure of PKS provided mechanical interlocking for reducing the volume loss and maintaining the hardness of XNBR composites when subjected to force. According to the results, PKS could be fully replaced with CB as reinforcement in rubber composites since it provides high abrasion resistance and hardness to the vulcanize.

However, it is noteworthy that replacing CB with biochar typically degrades the reinforcement properties of rubber composites owing to the much larger particle size of biochar and introducing localized stresses in the rubber composite. For this reason, "top-down" methods such as milling are used to reduce the size of biochar particles [174]. Peterson [175] made biochar from fast-growing Paulownia elongate and reduced its large particle size using co-milled with small amounts of silica (1%). Replacing half of the CB with silica-milled biochar caused equal or better elongation and toughness with little loss of tensile strength (less than 6%) compared to the 100% CB/NR composite as a control. In another paper, Peterson [176] produced biochar from coppiced hardwoods Populus tremuloides and Paulownia elongate. The silica-milled biochar was used as an alternative to CB in SBR/NR composites. Concerning the control sample with 100% CB, replacing 30% of the CB with biochar from both feedstocks increased elongation and toughness properties with no loss in tensile strength. Table 9 summarises the effect of biochar incorporation on rubber composites' mechanical characteristics.

5. Recycled carbon black (generated from discarded tire)

At the beginning of the 20th century, rubber production and consumption and the dynamic development of the rubber industry are increasing rapidly worldwide. Since the number of vehicles is continuously growing all over the world, the maximum percentage of rubbers (about 68%) is utilized in the tire industry (Fig. 16a) [182]. This high rubber consumption in the tire industry produces huge waste tires yearly. Fig. 16b shows the current global waste rubber generation. As can be seen in the figure, the largest amount of waste rubber (31%) is produced by North America, whereas Asia (excluding Japan) has the minimum of scrap rubber (19%) [183]. Disposing of these waste rubbers causes numerous environmental concerns, making it a challenging issue in the twenty-first century.

Since the tires are produced by chemical cross-linking of polymer-filler materials, recycling is challenging. Sathiskumar et al. [184] explained the various disposal techniques for waste rubber products, including reclaiming, combustion, retreading, grinding and pyrolysis. They reported that pyrolysis is a promising recycling approach compared with other disposal techniques since it converts waste rubber into value-added products. For example, the pyrolysis of automotive waste tires makes it possible to transfer hundreds of tons of waste tires into gaseous, liquid, steel wire, and carbon-rich solid (RCB) fractions, mainly including carbon fractions from conventional CB and inorganic ingredients utilized during tire building [185]. The utilization of recovered carbon black (rCB) generated from the pyrolysis of waste tires has drawn great attention in recent years as an alternative for commercial CB. Incorporating this filler into the rubber matrix improves the mechanical and physical properties of filled-rubber composites. Nevertheless, rCB possesses poor reinforcement features with respect to commercial CB when used for tire tread rubber [186].

Lately, Zhang et al. [187] examined the replacement of commercial CB N330 with rCB (50% and 100%) in NR compounds used in tire rubber composites. Additionally, they evaluated the effect of a novel coupling agent, sodium (Z)-4-((4-aminophenyl) amino)-4-oxobut-2-enoate, on the reinforcement properties of NR composites. The results showed that by substituting CB N330 with rCB, the modulus at 100% and 300% strain (M100 and M300) and the tensile strength decreased due to the poor reinforcement characteristic of rCB. In the presence of a coupling agent, the dispersion of rCB improved, and the bound rubber content of filled NR composites increased. Moreover, the coupling agent improved the tensile strength of the M100 and M300 strains of NR vulcanizates while it reduced the Payne effect and the rolling resistance of rCB-filled NR composites. These findings could be associated with building a bridge between rCB and NR by coupling agent, which increases the

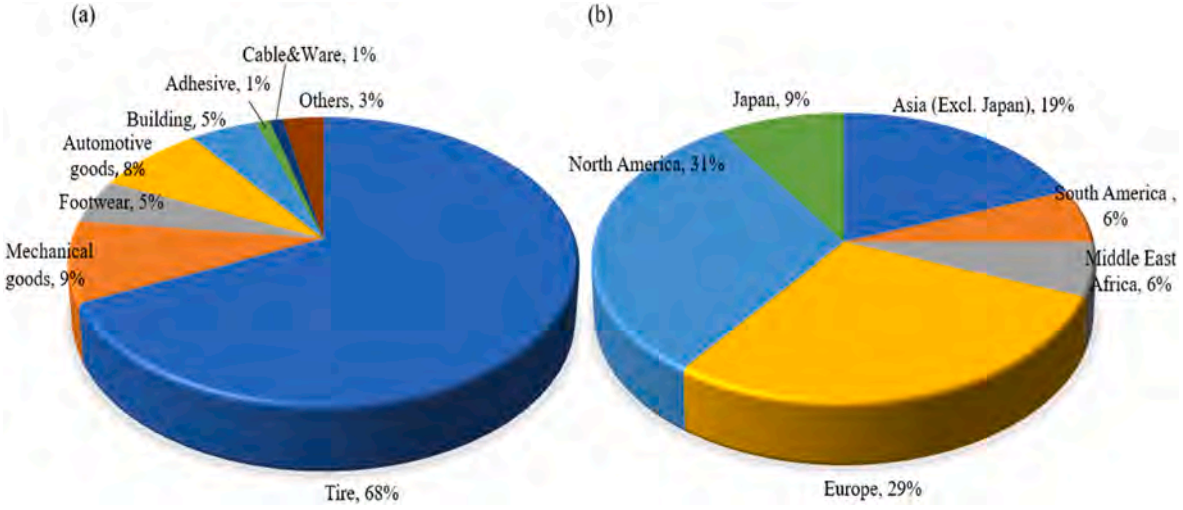

Fig. 16. (a) The percentages of rubber consumption in various industries; (b) the global production of waste rubber.

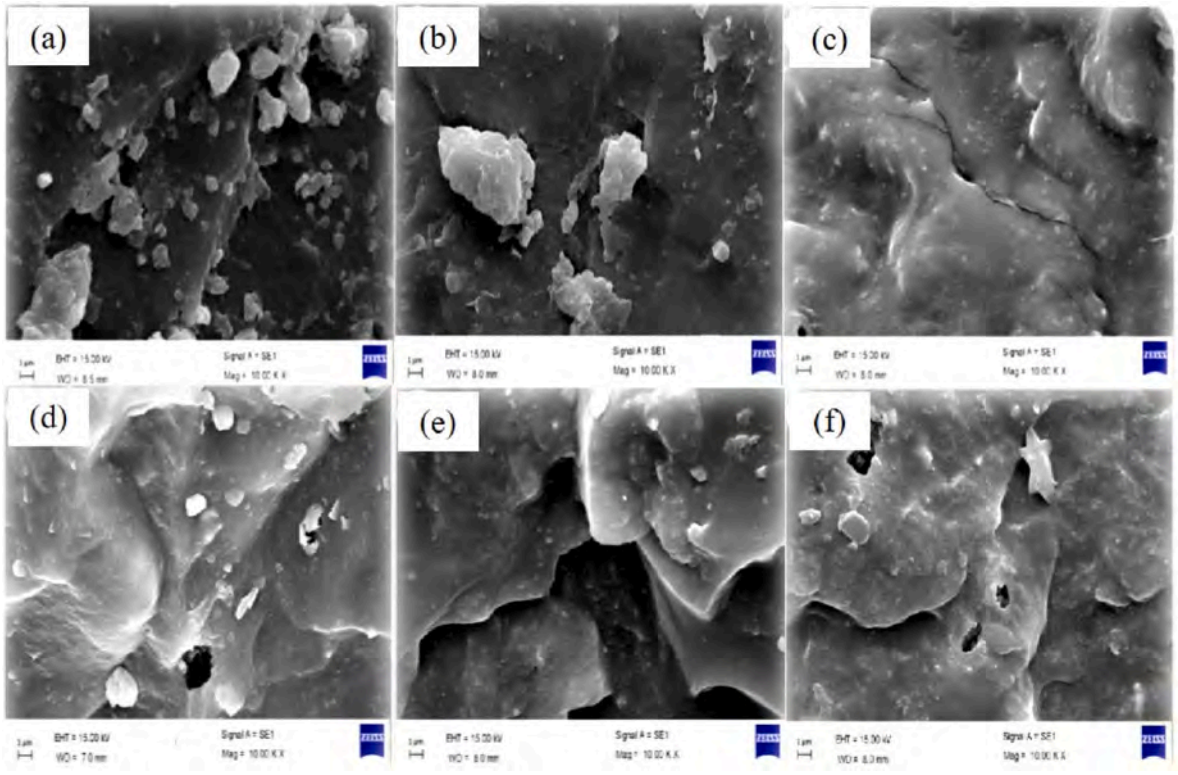

Fig. 17. SEM micrograph of SiO_2/NR composites in the presence of various *r*-NR, (a) *r*-NR(0); (b) 20 wt% *r*-NR; (c) 30 wt% *r*-NR; (d) 40 wt% *r*-NR; (e) 50 wt% *r*-NR and (f) 60 wt% *r*-NR, Reprinted from Ref. [191].

interaction between rCB and NR [188]. Araujo-Morera [189] used a cryo-grinding process and chemical treatment (sulfuric acid) for modification of the ground tire rubber surface (GTR) to improve the compatibility between the waste material and the rubber matrix. By introducing 10 phr modified-GTR into the SBR matrix, the tensile strength and elongation at the break increased by 115% and 761%, respectively. These achievements can be explained by the interaction between the polar functional groups on the surface of modified-GTR with the SBR matrix resulting in the adhesion between phases and improved mechanical performance of the modified-GTR/SBR composite.

In another study, Jovičić et al. [190] investigated the impact of recycled CB on the curing process and mechanical properties of vulcanized NR as a substitution for commercial CB (N330). Loading a high content of rCB resulted in a postponement of the vulcanization reaction and an increased curing time. In addition, the mechanical characteristics of the rCB/NR composite decreased due to a reduction in cross-link density. Therefore, rCB was found unsuitable for the complete substitution of CB. However, it could be blended with commercial CB at less than 15 phr (up to 50%) content in the NR matrix. Ghorai et al. [191] studied the effect of devulcanized rubber (*r*-NR) loading (20–60 wt%) on the mechanical properties of silica/NR composites (as a control formulation). Increasing the content of *r*-NR showed a significant improvement in the elongation at break, tensile strength, tear strength, and abrasion loss compared to the control formulation. These improved properties in NR/r-NR/SiO_2 composites were attributed to the increased vulcanizate cross-link density, which restricted the mobility of rubber chains. The enhanced rubber-silica interaction also facilitated better silica dispersion, as evidenced by the homogenous distribution of the silica filler in the NR matrix observed in the SEM images (Fig. 17). Based on the results, the authors reported that the optimum content of *r*-NR was 40 phr for SiO_2/NR composite.

Table 10 presents the main mechanical properties of rubber composites filled with pyrolyzed waste tires.

6. Conclusions

The addition of fillers into rubber composites has a significant effect on their properties and performance. Conventional fillers, such as CB and silica, have been extensively used in rubber composites due to their excellent reinforcing properties. However, their production processes often have negative environmental impacts, including energy consumption, greenhouse gas emissions, and the depletion of non-renewable resources. To address these concerns, extensive studies have been conducted to explore alternative fillers that are more cost-effective and environmentally friendly.

The current development of bio-based fillers (biofiller) for rubber composites has shown promising results. Incorporating renewable and sustainable biofillers into rubber composites offers a great opportunity to enhance rubber-based products' sustainability while maintaining or improving their performance properties. These biofillers, derived from renewable sources such as plant-based materials, agricultural waste, etc., provide excellent reinforcement properties and reduce dependence on fossil fuel-derived materials. The addition of biofillers into rubber composites can contribute to circular economy principles by reducing waste generation and promoting resource conservation. This shift towards biofillers also aligns with the goals of reducing carbon emissions and mitigating environmental impact, contributing to a greener future. Furthermore, the biodegradability and recyclability of rubber composites can be improved, further reducing their impact on the environment and enabling the development of sustainable end-of-life solutions. Despite their eco-friendly nature, these biofillers can positively affect rubber composites' mechanical properties and performance characteristics. They can improve attributes like tensile strength, tear resistance, and wear resistance, which are essential for various rubber products across industries.

To conclude, the addition of renewable and sustainable biofillers enables a more sustainable approach to rubber composite production, promoting a greener and more responsible future for the rubber

Table 10
Mechanical properties of recycled CB-filled rubber composites.

Rubber composites	Filler loading	Mechanical characteristics	rCB Suppliers/Modifier	Ref
rCB/CB (N330)/ NR	rCB: 7.5 phr CB: 22.5 phr	- Tensile strength (MPa): 15.89 - Elongation at break (%): 343.6 - Hardness (∘ Sh A): 64 - Modulus 300% (MPa): 12.34	Purchased from Eko Tire, Belgrade, with a carbon content of 71.58 wt%	[190]
	rCB: 15 phr CB: 15 phr	- Tensile strength (MPa): 13.79 - Elongation at break (%): 356.7 - Hardness (∘ Sh A): 62 - Modulus 300% (MPa): 10.21		
rCB(XS660)/ CB (N330)/ NR	rCB: 25 phr CB: 25 phr	- Tensile strength (MPa): 26.8 - Elongation at break (%): 451 - Tear strength (KN/m): 61 - Modulus 300% (MPa): 15.8	Provided by Shanghai Rubber Light International Trading Company/Coupling agent (1 phr)	[187]
	rCB: 50 phr	- Tensile strength (MPa): 26.0 - Elongation at break (%): 429 - Tear strength (KN/m): 55 - Modulus 300% (MPa): 15.7	Provided by Shanghai Rubber Light International Trading Company/Coupling agent (2 phr)	
rCB/SBR	rCB: 10 phr	- Tensile strength (MPa): 2.8 ± 0.2 - Elongation at break (%): 1187 ± 146 - Modulus 500% (MPa): 0.94 ± 0.03 - Hardness (∘ Sh A): 27	Supplied by Signus/ Chemical treatments with H_2SO_4	[189]
rCB/NRL	rCB: 50 phr	- Tensile strength (MPa): 24.28 - Elongation at break (%): 596 - Tear strength (KN/m): 83 - Hardness (shore A): 55 - Resilience (%): 64.98 - Abrasion (cm^{-3}): 0.189	Produced in laboratory pyrolysis with Heating rate: 60 K/h Temperature: 450 °C C%: 82.02	[192]
rCB/CB (N234)/ SSBR/BR	rCB: 20 phr CB: 20 phr	- Tensile strength (MPa): 19.4 - Elongation at break (%): 431 - Modulus 100% (MPa): 2.8 - Modulus 300% (MPa): 12.4	Provided by Shanghai Rubber Light International Trading Company/liquid polyisoprene	[193]

rCB: Recycled carbon black; **CB**: Carbon black; **SBR**: Styrene-Butadiene Rubber; **SSBR**: Solution-polymerized styrene-butadiene rubber; **NR**: Natural rubber; **NRL**: Natural rubber latex; **BR**: Butadiene rubber; **H_2SO_4**: sulfuric acid.

industry. Nevertheless, further research is needed to explore and optimize the processing techniques, compatibility, and performance of these fillers in different rubber formulations.

CRediT authorship contribution statement

Mehran Dadkhah: Conceptualization, Data curation, Investigation, Validation, Writing – original draft. **Massimo Messori:** Conceptualization, Supervision, Validation, Visualization, Writing – review & editing.

Declaration of competing interest

The authors declare that they have no known competing financial interests or personal relationships that could have appeared to influence the work reported in this paper.

Data availability

Data will be made available on request.

References

[1] N. Srirachya, T. Kobayashi, K. Roy, K. Boonkerd, Thermoreversible cross-linking of Maleated natural rubber with glycerol, J. Elastomers \& Plast. 51 (2019) 406–420, https://doi.org/10.1177/0095244318790616.
[2] D. Basu, A. Das, K.W. Stöckelhuber, U. Wagenknecht, G. Heinrich, Advances in layered double hydroxide (LDH)-Based elastomer composites, Prog. Polym. Sci. 39 (2014) 594–626, https://doi.org/10.1016/j.progpolymsci.2013.07.011.
[3] B.P. Chang, A. Gupta, R. Muthuraj, T.H. Mekonnen, Bioresourced fillers for rubber composite sustainability: current development and future opportunities, Green Chem. 23 (2021) 5337–5378, https://doi.org/10.1039/D1GC01115D.
[4] Y. Liu, Q. Zhou, Q. Lu, C. Han, Z. Zhou, Z. Liang, R. Liu, Y. Nie, Reinforcement and toughening of rubber by bridging graphene and nanosilica, J. Inorg. Organomet. Polym. Mater. 30 (2020) 337–348, https://doi.org/10.1007/s10904-019-01192-2.
[5] K. Roy, S.C. Debnath, P. Potiyaraj, A critical review on the utilization of various reinforcement modifiers in filled rubber composites, J. Elastomers \& Plast. 52 (2020) 167–193, https://doi.org/10.1177/0095244319835869.
[6] R. Zafarmehrabian, S. Taghvaei Gangali, M.H.R. Ghoreishy, The effects of silica/carbon black ratio on the dynamic properties of the tread compounds in truck tires, E-journal Chem. 9 (2012) 1102–1112.
[7] J. Diani, B. Fayolle, P. Gilormini, A review on the Mullins effect, Eur. Polym. J. 45 (2009) 601–612, https://doi.org/10.1016/j.eurpolymj.2008.11.017.
[8] M. Gonzales-Fernandes, A.C.G. Bastos, F.J. Esper, F.R. Valenzuela-Diaz, H. Wiebeck, Improvement of mechanical properties in natural rubber with organic fillers. Characterization of Minerals, Metals, and Materials, Springer International Publishing, Cham, 2016, ISBN 978-3-319-48210-1, pp. 623–627.
[9] L. Mullins, Effect of stretching on the properties of rubber, Rubber Chem. Technol. 21 (1948) 281–300, https://doi.org/10.5254/1.3546914.
[10] C. Ma, T. Ji, C.G. Robertson, R. Rajeshbabu, J. Zhu, Y. Dong, Molecular insight into the Mullins effect: irreversible disentanglement of polymer chains revealed by molecular dynamics simulations, Phys. Chem. Chem. Phys. 19 (2017) 19468, 19477.
[11] H. Zhang, A.K. Scholz, F. Vion-Loisel, Y. Merckel, M. Brieu, H. Brown, S. Roux, E. J. Kramer, C. Creton, Opening and closing of nanocavities under cyclic loading in a soft nanocomposite probed by real-time small-angle X-ray scattering, Macromolecules 46 (2013) 900–913, https://doi.org/10.1021/ma302325w.
[12] T.-T. Mai, K. Okuno, K. Tsunoda, K. Urayama, Anisotropic stress-softening effect on fast dynamic crack in filler-reinforced elastomers, Mech. Mater. 155 (2021) 103786, https://doi.org/10.1016/j.mechmat.2021.103786.
[13] J. Neethirajan, A.R. Parathodika, G.-H. Hu, K. Naskar, Functional rubber composites based on silica-silane reinforcement for green tire application: the state of the art, Funct. Compos. Mater. 3 (2022) 7, https://doi.org/10.1186/s42252-022-00035-7.
[14] S. Tang, J. Li, R. Wang, J. Zhang, Y. Lu, G.-H. Hu, Z. Wang, L. Zhang, Current trends in bio-based elastomer materials, SusMat 2 (2022) 2–33, https://doi.org/10.1002/sus2.45.
[15] K. Roy, S.C. Debnath, L. Tzounis, A. Pongwisuthiruchte, P. Potiyaraj, Effect of various surface treatments on the performance of jute fibers filled natural rubber (NR) composites, Polymers (Basel) 12 (2020), https://doi.org/10.3390/polym12020369.
[16] P. Sahu, M.K. Gupta, A review on the properties of natural fibres and its bio-composites: effect of alkali treatment, Proc. Inst. Mech. Eng. Part L J. Mater. Des. Appl. 234 (2020) 198–217, https://doi.org/10.1177/1464420719875163.
[17] J. Miedzianowska, M. Masłowski, P. Rybiński, K. Strzelec, Properties of chemically modified (selected silanes) lignocellulosic filler and its application in natural rubber biocomposites, Materials (Basel) 13 (2020), https://doi.org/10.3390/ma13184163.

[18] Z. Tang, C. Zhang, Q. Wei, P. Weng, B. Guo, Remarkably improving performance of carbon black-filled rubber composites by incorporating MoS2 nanoplatelets, Compos. Sci. Technol. 132 (2016) 93–100, https://doi.org/10.1016/j.compscitech.2016.07.001.
[19] ICBA), I.C.B.A. No Title, Carbon Black User's Guid (2018). (Accessed 13 July 2023).
[20] X. Shi, S. Sun, A. Zhao, H. Zhang, M. Zuo, Y. Song, Q. Zheng, Influence of carbon black on the Payne effect of filled natural rubber compounds, Compos. Sci. Technol. 203 (2021) 108586, https://doi.org/10.1016/j.compscitech.2020.108586.
[21] R. Zafarmehrabian, S.T. Gangali, M.H.R. Ghoreishy, M. Davallu, The effects of silica/carbon black ratio on the dynamic properties of the tread compounds in truck tires, E-Journal Chem. 9 (2012) 1102–1112, https://doi.org/10.1155/2012/571957.
[22] A. Kato, Y. Ikeda, S. Kohjiya, Reinforcement mechanism of carbon black (CB) in natural rubber vulcanizates: relationship between CB aggregate and network structure and viscoelastic properties, Polym. Plast. Technol. Eng. 57 (2018) 1418–1429, https://doi.org/10.1080/03602559.2017.1381257.
[23] J. Chanda, N. Mishra, T. Dolui, P. Ghosh, R. Mukhopadhyay, Fatigue crack growth behavior and morphological analysis of natural rubber compounds with varying particle size and structure of carbon black, Polym. Eng. \& Sci. 62 (2022) 743–757, https://doi.org/10.1002/pen.25881.
[24] W. Fu, L. Wang, J. Huang, C. Liu, W. Peng, H. Xiao, S. Li, Mechanical properties and Mullins effect in natural rubber reinforced by grafted carbon black, Adv. Polym. Technol. 2019 (2019) 4523696, https://doi.org/10.1155/2019/4523696.
[25] R. Diaz, J. Diani, P. Gilormini, Physical interpretation of the Mullins softening in a carbon-black filled SBR, Polymer (Guildf). 55 (2014) 4942–4947, https://doi.org/10.1016/j.polymer.2014.08.020.
[26] Z. Li, H. Xu, X. Xia, Y. Song, Q. Zheng, Energy dissipation accompanying Mullins effect of nitrile butadiene rubber/carbon black nanocomposites, Polymer (Guildf). 171 (2019) 106–114, https://doi.org/10.1016/j.polymer.2019.03.043.
[27] J. Zhou, W. Wang, Y. Song, Q. Zheng, Effect of ionic liquid on structure and properties of carbon black filled natural rubber vulcanizates, Compos. Part A Appl. Sci. Manuf. 167 (2023) 107432, https://doi.org/10.1016/j.compositesa.2023.107432.
[28] A. Vayyaprontavida Kaliyathan, A.V. Rane, M. Huskic, K. Kanny, M. Kunaver, N. Kalarikkal, S. Thomas, The effect of adding carbon black to natural rubber/butadiene rubber blends on curing, morphological, and mechanical characteristics, J. Appl. Polym. Sci. 139 (2022) 51967, https://doi.org/10.1002/app.51967.
[29] S.K. Srivastava, Y.K. Mishra, Nanocarbon reinforced rubber nanocomposites: detailed insights about mechanical, dynamical mechanical properties, Payne, and mullin effects, Nanomaterials 8 (2018), https://doi.org/10.3390/nano8110945.
[30] S. Mondal, P. Das, S. Ganguly, R. Ravindren, S. Remanan, P. Bhawal, T.K. Das, N. C. Das, Thermal-air ageing treatment on mechanical, electrical, and electromagnetic interference shielding properties of lightweight carbon nanotube based polymer nanocomposites, Compos. Part A Appl. Sci. Manuf. 107 (2018) 447–460, https://doi.org/10.1016/j.compositesa.2018.01.025.
[31] P.S. Thomas, A.A. Abdullateef, M.A. Al-Harthi, A.A. Basfar, S. Bandyopadhyay, M. A. Atieh, S.K. De, Effect of phenol functionalization of carbon nanotubes on properties of natural rubber nanocomposites, J. Appl. Polym. Sci. 124 (2012) 2370–2376, https://doi.org/10.1002/app.35274.
[32] F. Cataldo, O. Ursini, G. Angelini, MWCNTs elastomer nanocomposite, Part 1: the addition of MWCNTs to a natural rubber-based carbon black-filled rubber compound, Fullerenes, Nanotub. Carbon Nanostructures 17 (2009) 38–54, https://doi.org/10.1080/15363830802515907.
[33] J. Xu, S. Li, Y. Li, X. Ta, Preparation, morphology and properties of natural rubber/carbon black/multi-walled carbon nanotubes conductive composites, J. Mater. Sci. Mater. Electron. 27 (2016) 9531–9540, https://doi.org/10.1007/s10854-016-5005-4.
[34] L. Gu, H. Nan, R. Xing, G. Pan, Y. Wang, X. Ge, Mechanical and thermal performances of styrene butadiene rubber nanocomposites with boron nitride nanosheets, carbon nanotubes, and the hybrid filler system, Polym. Compos. 44 (2023) 480–491, https://doi.org/10.1002/pc.27111.
[35] O. Al-Hartomy, A. Al-Ghamdi, S.F. Al Said, N. Dishovsky, M. Mihaylov, M. Ivanov, D. Zaimova, Comparison of the dielectric thermal properties and dynamic mechanical thermal properties of natural rubber-based composites comprising multiwall carbon nanotubes and graphene nanoplatelets, Fullerenes, Nanotub. Carbon Nanostructures 23 (2015) 1001–1007, https://doi.org/10.1080/1536383X.2015.1004572.
[36] S. Matchawet, A. Kaesaman, P. Bomlai, C. Nakason, Effects of multi-walled carbon nanotubes and conductive carbon black on electrical, dielectric, and mechanical properties of epoxidized natural rubber composites, Polym. Compos. 38 (2017) 1031–1042, https://doi.org/10.1002/pc.23666.
[37] F. Teng, J. Wu, B. Su, Y. Wang, Enhanced adhesion friction behaviors of nature rubber composites by applications of carbon nanotube: experiment and molecular insight, Tribol. Int. 181 (2023) 108333, https://doi.org/10.1016/j.triboint.2023.108333.
[38] C. Lee, X. Wei, J.W. Kysar, J. Hone, Measurement of the elastic properties and intrinsic strength of monolayer graphene, Science (80) 321 (2008) 385–388, https://doi.org/10.1126/science.1157996.
[39] K.I. Bolotin, K.J. Sikes, Z. Jiang, M. Klima, G. Fudenberg, J. Hone, P. Kim, H. L. Stormer, Ultrahigh electron mobility in suspended graphene, Solid State Commun 146 (2008) 351–355, https://doi.org/10.1016/j.ssc.2008.02.024.
[40] A.S. Sethulekshmi, A. Saritha, K. Joseph, A comprehensive review on the recent advancements in natural rubber nanocomposites, Int. J. Biol. Macromol. 194 (2022) 819–842, https://doi.org/10.1016/j.ijbiomac.2021.11.134.
[41] H. Kang, Y. Tang, L. Yao, F. Yang, Q. Fang, D. Hui, Fabrication of graphene/natural rubber nanocomposites with high dynamic properties through convenient mechanical mixing, Compos. Part B Eng. 112 (2017) 1–7, https://doi.org/10.1016/j.compositesb.2016.12.035.
[42] D. An, Y. Cui, R. He, J. Chen, X. Duan, J. Li, Y. Liu, Y. Liu, H. Yu, C. Wong, Improved interfacial interactions of modified graphene oxide/natural rubber composites with the low heat build-up and good mechanical property for the green tire application, Polym. Compos. (2023), https://doi.org/10.1002/pc.27444.
[43] H. Liu, L. Yang, X. Liu, J.-P. Cao, J. Zhang, Z. Luo, Z. Gao, Silicon dioxide nanoparticle decorated graphene with excellent dispersibility in natural rubber composites via physical mixing for application in green tires, Compos. Part B Eng. 258 (2023) 110700, https://doi.org/10.1016/j.compositesb.2023.110700.
[44] Q. Li, G. Lin, S. Chen, L. Zhang, Y. Song, C. Geng, S. Qu, Y. Jing, F. Liu, Z. Liang, Enhancing mechanical performance and wet-skid resistance of emulsion styrene butadiene rubber/natural rubber latex composites via in-situ hybridization of silanized graphene oxide and silica, J. Appl. Polym. Sci. 139 (2022) 52083, https://doi.org/10.1002/app.52083.
[45] V. Bijina, P.J. Jandas, J. Jose, M.A. N, A. K, H. John, Tailoring of performance characteristics of green tyre tread formulation using thermally exfoliated graphite/carbon black binary filler system via scalable and competent method, Res. Sq (2022).
[46] M.N. Alam, V. Kumar, P. Potiyaraj, D.-J. Lee, J. Choi, Mutual dispersion of graphite–silica binary fillers and its effects on curing, mechanical, and aging properties of natural rubber composites, Polym. Bull. 79 (2022) 2707–2724, https://doi.org/10.1007/s00289-021-03608-x.
[47] K.P. Rajan, A. Gopanna, R. Theravalappil, E.A.M. Abdelghani, S.P. Thomas, Partial replacement of carbon black with graphene in natural rubber/butadiene rubber based tire compound: investigation of critical properties, J. Polym. Res. 29 (2022) 76, https://doi.org/10.1007/s10965-021-02871-w.
[48] J.R. Innes, R.J. Young, D.G. Papageorgiou, Graphene nanoplatelets as a replacement for carbon black in rubber compounds, Polymers (Basel) 14 (2022), https://doi.org/10.3390/polym14061204.
[49] K. Damampai, S. Pichaiyut, S. Mandal, S. Wießner, A. Das, C. Nakason, Internal polymerization of epoxy group of epoxidized natural rubber by ferric chloride and formation of strong network structure, Polymers (Basel) 13 (2021), https://doi.org/10.3390/polym13234145.
[50] S. Song, Y. Zhang, Carbon nanotube/reduced graphene oxide hybrid for simultaneously enhancing the thermal conductivity and mechanical properties of styrene -butadiene rubber, Carbon N. Y. 123 (2017) 158–167, https://doi.org/10.1016/j.carbon.2017.07.057.
[51] Y. Nakaramontri, C. Kummerlöwe, C. Nakason, N. Vennemann, The effect of surface functionalization of carbon nanotubes on properties of natural rubber/carbon nanotube composites, Polym. Compos. 36 (2015) 2113–2122, https://doi.org/10.1002/pc.23122.
[52] Y. Nakaramontri, C. Nakason, C. Kummerlöwe, N. Vennemann, Effects of in-situ functionalization of carbon nanotubes with bis(triethoxysilylpropyl) tetrasulfide (TESPT) and 3-aminopropyltriethoxysilane (APTES) on properties of epoxidized natural rubber–carbon nanotube composites, Polym. Eng. \& Sci. 55 (2015) 2500–2510, https://doi.org/10.1002/pen.24140.
[53] M. Li, W. Tu, X. Chen, H. Wang, J. Chen, NR/SBR composites reinforced with organically functionalized MWCNTs: simultaneous improvement of tensile strength and elongation and enhanced thermal stability, J. Polym. Eng. 36 (2016) 813–818, https://doi.org/10.1515/polyeng-2015-0136.
[54] S. Mondal, D. Khastgir, Elastomer reinforcement by graphene nanoplatelets and synergistic improvements of electrical and mechanical properties of composites by hybrid nano fillers of graphene-carbon black & graphene-MWCNT, Compos. Part A Appl. Sci. Manuf. 102 (2017) 154–165, https://doi.org/10.1016/j.compositesa.2017.08.003.
[55] X. Zhang, J. Wang, H. Jia, B. Yin, L. Ding, Z. Xu, Q. Ji, Polyvinyl pyrrolidone modified graphene oxide for improving the mechanical, thermal conductivity and solvent resistance properties of natural rubber, RSC Adv. 6 (2016) 54668–54678, https://doi.org/10.1039/C6RA11601A.
[56] C. Zhang, T. Zhai, Y. Dan, L.-S. Turng, Reinforced natural rubber nanocomposites using graphene oxide as a reinforcing agent and their in situ reduction into highly conductive materials, Polym. Compos. 38 (2017) E199–E207, https://doi.org/10.1002/pc.23972.
[57] S. Dul, L. Fambri, C. Merlini, G.M.O. Barra, M. Bersani, L. Vanzetti, A. Pegoretti, Effect of graphene nanoplatelets structure on the properties of acrylonitrile–butadiene–styrene composites, Polym. Compos. 40 (2019) E285–E300, https://doi.org/10.1002/pc.24645.
[58] M.G. Maya, J. Abraham, P.M. Arif, G. Moni, J.J. George, S.C. George, S. Thomas, A comprehensive study on the impact of RGO/MWCNT hybrid filler reinforced Polychloroprene rubber multifunctional nanocomposites, Polym. Test. 87 (2020) 106525, https://doi.org/10.1016/j.polymertesting.2020.106525.
[59] S. Jovanović, S. Samaržija-Jovanović, G. Marković, V. Jovanović, T. Adamović, M. Marinović-Cincović, Mechanical properties and thermal aging behaviour of polyisoprene/polybutadiene/styrene-butadiene rubber ternary blend reinforced with carbon black, Compos. Part B Eng. 98 (2016) 126–133, https://doi.org/10.1016/j.compositesb.2016.04.060.
[60] F. Shahamatifard, D. Rodrigue, K.-W. Park, S. Frikha, F. Mighri, Synergistic effect between graphene nanoplatelets and carbon black to improve the thermal and

mechanical properties of natural rubber nanocomposites, Polym. Technol. Mater. 61 (2022) 1578–1592, https://doi.org/10.1080/25740881.2022.2071162.
[61] L. Kong, F. Li, F. Wang, Y. Miao, X. Huang, H. Zhu, Y. Lu, High-performing multi-walled carbon nanotubes/silica nanocomposites for elastomer application, Compos. Sci. Technol. 162 (2018) 23–32, https://doi.org/10.1016/j.compscitech.2018.04.008.
[62] Nanjing Hao, Laifeng Li, F. Tang, Shape matters when engineering mesoporous silica-based nanomedicines, Biomater. Sci. 4 (2016) 575–591.
[63] N. Hao, L. Li, F. Tang, Roles of particle size, shape and surface chemistry of mesoporous silica nanomaterials on biological systems, Int. Mater. Rev. 62 (2017) 57–77, https://doi.org/10.1080/09506608.2016.1190118.
[64] S. Salina Sarkawi, Wisut Kaewsakul, Kannika Sahakaro, Wilma K. Dierkes, J. W. Noordermeer, A review on reinforcement of natural rubber by silica fillers for use in low-rolling resistance tyres, J. rubber Res. 18 (2015).
[65] K.W. Stöckelhuber, A.S. Svistkov, A.G. Pelevin, G. Heinrich, Impact of filler surface modification on large scale mechanics of styrene butadiene/silica rubber composites, Macromolecules 44 (2011) 4366–4381, https://doi.org/10.1021/ma1026077.
[66] B. Shoul, Y. Marfavi, B. Sadeghi, E. Kowsari, P. Sadeghi, S. Ramakrishna, Investigating the potential of sustainable use of green silica in the green tire industry: a review, Environ. Sci. Pollut. Res. 29 (2022) 51298–51317, https://doi.org/10.1007/s11356-022-20894-8.
[67] J. Neethirajan, T.S. Natarajan, S. Wiessner, K. Naskar, A. Das, Tuning the mechanical properties of MgO filled epichlorohydrin elastomer composites through in-situ alteration of filler structure using water as stimulus, Mater. Today Commun. 26 (2021) 102116, https://doi.org/10.1016/j.mtcomm.2021.102116.
[68] S. Sattayanurak, K. Sahakaro, W. Kaewsakul, W.K. Dierkes, L.A.E.M. Reuvekamp, A. Blume, J.W.M. Noordermeer, Synergistic effect by high specific surface area carbon black as secondary filler in silica reinforced natural rubber tire tread compounds, Polym. Test. 81 (2020) 106173, https://doi.org/10.1016/j.polymertesting.2019.106173.
[69] Z.A.S.A. Salim, A. Hassan, H. Ismail, A review on hybrid fillers in rubber composites, Polym. Plast. Technol. Eng. 57 (2018) 523–539, https://doi.org/10.1080/03602559.2017.1329432.
[70] X. Gao, W. Yang, C. Wang, X. Tian, Study on properties of carbon-coated silica prepared by polymer pyrolysis reinforced rubber composites, Polym. Test. 110 (2022) 107583, https://doi.org/10.1016/j.polymertesting.2022.107583.
[71] X. Zheng, S.K. Song, Z. Zhou, X. Jiang, Y. Sui, M. Che, Q. Xu, Y. Wang, S. Zhao, L. Li, Effect of silica dispersed by special dispersing agents with green strategy on tire rolling resistance and energy consumption, J. Appl. Polym. Sci. 139 (2022) e52933, https://doi.org/10.1002/app.52933.
[72] X. Wang, Z. Luo, Y. Xu, J. Zhong, H. Zhang, J. Liang, Preparation and performance of natural rubber latex treatment for silica filled natural rubber composites, J. Appl. Polym. Sci. 140 (2023) e53966, https://doi.org/10.1002/app.53966.
[73] M. Zielińska, R. Seyger, W.K. Dierkes, D. Bielinski, J.W.M.N. Silane, Grafted natural rubber and its compatibilization effect on silica-reinforced rubber tire compounds, Express Polym Lett 11 (2017) 1003–1022.
[74] M. Maciejewska, A. Sowińska-Baranowska, Bromide and chloride ionic liquids applied to enhance the vulcanization and performance of natural rubber biocomposites filled with nanosized silica, Nanomaterials 12 (2022), https://doi.org/10.3390/nano12071209.
[75] M.N. Alam, V. Kumar, S.C. Debnath, T. Jeong, S.-S. Park, Naturally abundant silica-kaolinite mixed minerals as an outstanding reinforcing filler for the advancement of natural rubber composites, J. Polym. Res. 30 (2023) 59, https://doi.org/10.1007/s10965-022-03424-5.
[76] M.N. Kalat, M. Razzaghi-Kashani, The role of reduced graphene oxide as a secondary filler in improving the performance of silica-filled styrene-butadiene rubber compounds, Polym. J. 54 (2022) 355–365, https://doi.org/10.1038/s41428-021-00570-3.
[77] Y. Fan, G.D. Fowler, M. Zhao, The past, present and future of carbon black as a rubber reinforcing filler – a review, J. Clean. Prod. 247 (2020) 119115, https://doi.org/10.1016/j.jclepro.2019.119115.
[78] T.R. Mohanty, V. Bhandari, A.K. Chandra, P.K. Chattopadhyay, S. Chattopadhyay, Role of calcium stearate as a dispersion promoter for new generation carbon black-organoclay based rubber nanocomposites for tyre application, Polym. Compos. 34 (2013) 214–224, https://doi.org/10.1002/pc.22403.
[79] A. Hosseinmardi, P.K. Annamalai, L. Wang, D. Martin, N. Amiralian, Reinforcement of natural rubber latex using lignocellulosic nanofibers isolated from spinifex grass, Nanoscale 9 (2017) 9510–9519, https://doi.org/10.1039/c7nr02632c.
[80] A. Hosseinmardi, P.K. Annamalai, B. Martine, J. Pennells, D.J. Martin, N. Amiralian, Facile tuning of the surface energy of cellulose nanofibers for nanocomposite reinforcement, ACS Omega 3 (2018) 15933–15942, https://doi.org/10.1021/acsomega.8b02104.
[81] Razif Nordin, C.M.S. Said, H. Ismail, Properties of rice husk powder/natural rubber composite, Solid State Sci. Technol 15 (2007) 83–91.
[82] R. Abolghasemi, M. Haghighi, M. Solgi, A. Mobinikhaledi, Rapid synthesis of ZnO nanoparticles by waste thyme (Thymus Vulgaris L.), Int. J. Environ. Sci. Technol. 16 (2019) 6985–6990, https://doi.org/10.1007/s13762-018-2112-1.
[83] M. Sholeh, R. Rochmadi, H. Sulistyo, B. Budhijanto, Synthesis of precipitated silica from bagasse ash as reinforcing filler in rubber, IOP Conf. Ser. Mater. Sci. Eng. 778 (2020) 12012, https://doi.org/10.1088/1757-899X/778/1/012012.
[84] Elvis A. Okoronkwo, Patrick Ehi Imoisili, Olubayode, A. Smart, S.O. Olusunle, Development of silica nanoparticle from corn Cob ash, Adv. Nanoparticles 5 (2016) 135–139.
[85] N. Sapawe, M. Hanafi, Production of silica from agricultural waste, Arch. Org. Inorg. Chem. Sci. 3 (2018) 342–343.
[86] N. Surayah Osman, N. Sapawe, Waste material as an alternative source of silica precursor in silica nanoparticle synthesis – a review, Mater. Today Proc. 19 (2019) 1267–1272, https://doi.org/10.1016/j.matpr.2019.11.132.
[87] F. Farirai, M. Ozonoh, T.C. Aniokete, O. Eterigho-Ikelegbe, M. Mupa, B. Zeyi, M. O. Daramola, Methods of extracting silica and Silicon from agricultural waste ashes and application of the produced Silicon in solar cells: a mini-review, Int. J. Sustain. Eng. 14 (2021) 57–78, https://doi.org/10.1080/19397038.2020.1720854.
[88] B. Ravindran, N. Karmegam, A. Yuvaraj, R. Thangaraj, S.W. Chang, Z. Zhang, M. Kumar Awasthi, Cleaner production of agriculturally valuable benignant materials from industry generated bio-wastes: a review, Bioresour. Technol. 320 (2021) 124281, https://doi.org/10.1016/j.biortech.2020.124281.
[89] Addis Lemessa Jembere, S.W. Fanta, Studies on the synthesis of silica powder from rice husk ash as reinforcement filler in rubber tire tread part: replacement of commercial precipitated silica, SMR 20 (2017) 70.
[90] Potchanaporn Huabcharoen, Ekachai Wimolmala, Teerasak Markpin, N. Sombatsompop, Purification and characterization of silica from sugarcane bagasse ash as a reinforcing filler in natural rubber composites, BioResources 12 (2017) 1228–1245.
[91] Z.X. Ooi, H. Ismail, A.A. Bakar, Optimisation of oil palm ash as reinforcement in natural rubber vulcanisation: a comparison between silica and carbon black fillers, Polym. Test. 32 (2013) 625–630, https://doi.org/10.1016/j.polymertesting.2013.02.007.
[92] T.Z. Zaeimoedin, J. Clarke, A.K. Che Aziz, Improving the sustainability of 'green' tyre tread compound by using recovered silica filler, J. Rubber Res. 26 (2023) 37–46, https://doi.org/10.1007/s42464-023-00196-5.
[93] I.A. Rahman, P. Vejayakumaran, C.S. Sipaut, J. Ismail, C.K. Chee, Size-dependent physicochemical and optical properties of silica nanoparticles, Mater. Chem. Phys. 114 (2009) 328–332, https://doi.org/10.1016/j.matchemphys.2008.09.068.
[94] Y. Shen, Rice husk silica-derived nanomaterials for battery applications: a literature review, J. Agric. Food Chem. 65 (2017) 995–1004, https://doi.org/10.1021/acs.jafc.6b04777.
[95] M. Nazar, A. Yasar, S.A. Raza, A. Ahmad, R. Rasheed, M. Shahbaz, A.B. Tabinda, Techno-economic and environmental assessment of rice husk in comparison to coal and furnace oil as a boiler fuel, Biomass Convers. Biorefinery 13 (2023) 1671–1679, https://doi.org/10.1007/s13399-020-01238-3.
[96] M. Lolage, P. Parida, M. Chaskar, A. Gupta, D. Rautaray, Green silica: industrially scalable & sustainable approach towards achieving improved "nano filler – elastomer" interaction and reinforcement in tire tread compounds, Sustain. Mater. Technol. 26 (2020) e00232, https://doi.org/10.1016/j.susmat.2020.e00232.
[97] B.S. Parmar, N.P.S. Chauhan, A.S. Deuri, D. Vaidya, N.S. Chundawat, Study of physico-mechanical and dynamic mechanical properties of rice husk silica rubber compound replacing carbon black as a sustainable filler, AIP Conf. Proc. 2715 (2023) 20032, https://doi.org/10.1063/5.0134202.
[98] N. Choophun, N. Chaiammart, K. Sukthavon, C. Veranitisagul, A. Laobuthee, A. Watthanaphanit, G. Panomsuwan, Natural rubber composites reinforced with green silica from rice husk: effect of filler loading on mechanical properties, J. Compos. Sci. 6 (2022), https://doi.org/10.3390/jcs6120369.
[99] M. Shiva, M. Golmohammadi, F. Nouroozi, Extraction of silica from rice husk for rubber-cord adhesion systems of tire industry, Biomass Convers. Biorefinery (2023), https://doi.org/10.1007/s13399-023-03893-8.
[100] Narendra Singh Chundawat, Bhavani Shanker Parmar, Deuri, Arup Saha, Dilip Vaidya, Sapana Jadoun, Payam Zarrintaj, Mahmood Barani, N.P. S. Chauhan, Rice husk silica as a sustainable filler in the tire industry, Arab. J. Chem. 15 (2022) 104086.
[101] M. Qian, B. Zou, Z. Chen, W. Huang, X. Wang, B. Tang, Q. Liu, Y. Zhu, The influence of filler size and crosslinking degree of polymers on Mullins effect in filled NR/BR composites, Polymers (Basel) 13 (2021), https://doi.org/10.3390/polym13142284.
[102] M.-T. Le, Influence of nanosilica in mechanical property of natural rubber composite, in: *2018 4th International Conference On Green Technology And Sustainable Development (GTSD)*, IEEE, 2018, pp. 237–240.
[103] Midhun Dominic, Rani Joseph, PM Sabura Begum, Bipinbal Parambath Kanoth, Julie Chandra, S. Thomas, Green tire technology: effect of rice husk derived nanocellulose (RHNC) in replacing carbon black (CB) in natural rubber (NR) compounding, Carbohydr. Polym. 230 (2020) 115620.
[104] C.D. Midhun Dominic, A. Balan, K.V. Neenu, P.M. Sabura Begum, D. Joseph, P. Dileep, R. Joseph, M.J. Jaison, M. Mathew, C.S. Dhanya, et al., Sustainable Kerala rice husk ash for formulation of basic tyre tread: taking first step, Sustain. Mater. Technol. 32 (2022) e00427, https://doi.org/10.1016/j.susmat.2022.e00427.
[105] Z.X. Ooi, H. Ismail, A. Abu Bakar, Synergistic effect of oil palm ash filled natural rubber compound at low filler loading, Polym. Test. 32 (2013) 38–44, https://doi.org/10.1016/j.polymertesting.2012.09.007.
[106] R.K. Mishra, A. Sabu, S.K. Tiwari, Materials chemistry and the futurist eco-friendly applications of nanocellulose: status and prospect, J. Saudi Chem. Soc. 22 (2018) 949–978, https://doi.org/10.1016/j.jscs.2018.02.005.
[107] A. Dufresne, Nanocellulose: a new ageless bionanomaterial, Mater. Today 16 (2013) 220–227, https://doi.org/10.1016/j.mattod.2013.06.004.
[108] F. Deng, X. Ge, Y. Zhang, M.-C. Li, U.R. Cho, Synthesis and characterization of microcrystalline cellulose-graft-poly(Methyl Methacrylate) copolymers and their

application as rubber reinforcements, J. Appl. Polym. Sci. 132 (2015), https://doi.org/10.1002/app.42666.
[109] O. Somseemee, P. Sae-Oui, C. Siriwong, Reinforcement of surface-modified cellulose nanofibrils extracted from napier grass stem in natural rubber composites, Ind. Crops Prod. 171 (2021) 113881, https://doi.org/10.1016/j.indcrop.2021.113881.
[110] Natalie V. Weingart, A.M. Randall, Rubber compositions including cellulose esters and inorganic oxides, Google Patents, US Patent App 14/750 (2015), 023.
[111] K. Dhali, F. Daver, P. Cass, B. Adhikari, Surface modification of the cellulose nanocrystals through vinyl silane grafting, Int. J. Biol. Macromol. 200 (2022) 397–408, https://doi.org/10.1016/j.ijbiomac.2022.01.079.
[112] C. Zinge, B. Kandasubramanian, Nanocellulose based biodegradable polymers, Eur. Polym. J. 133 (2020) 109758, https://doi.org/10.1016/j.eurpolymj.2020.109758.
[113] Punyarat Jantachum, P.A. Phinyocheep, Simple method for extraction of cellulose nanocrystals from green Luffa cylindrica biomaterial and their characteristics, Polym. Int. 72 (2023) 243–251.
[114] P. Jantachum, B. Khumpaitool, S. Utara, Effect of silane coupling agent and cellulose nanocrystals loading on the properties of acrylonitrile butadiene rubber/natural rubber nanocomposites, Ind. Crops Prod. 195 (2023) 116407, https://doi.org/10.1016/j.indcrop.2023.116407.
[115] W. Jiang, P. Shen, J. Yi, L. Li, C. Wu, J. Gu, Surface modification of nanocrystalline cellulose and its application in natural rubber composites, J. Appl. Polym. Sci. 137 (2020) 49163, https://doi.org/10.1002/app.49163.
[116] W. Jiang, Z. Cheng, J. Wang, J. Gu, Modified nanocrystalline cellulose partially replaced carbon black to reinforce natural rubber composites, J. Appl. Polym. Sci. 139 (2022) 52057, https://doi.org/10.1002/app.52057.
[117] E.S. Abdul Rashid, N.B. Muhd Julkapli, W. Abdul Hadi Yehya, Reinforcement effect of nanocellulose on thermal stability of nitrile butadiene rubber (NBR) composites, J. Appl. Polym. Sci. 135 (2018) 46594, https://doi.org/10.1002/app.46594.
[118] G. Zhu, L. Giraldo Isaza, A. Dufresne, Cellulose nanocrystal-mediated assembly of graphene oxide in natural rubber nanocomposites with high electrical conductivity, J. Appl. Polym. Sci. 138 (2021) 51460, https://doi.org/10.1002/app.51460.
[119] J. Sun, X. Liu, Y. Liang, L. Wang, Y. Liu, The preparation of microcrystalline cellulose–NanoSiO2 hybrid materials and their application in tire tread compounds, J. Appl. Polym. Sci. 134 (2017), https://doi.org/10.1002/app.44796.
[120] P. Yu, H. He, Y. Luo, D. Jia, A. Dufresne, Reinforcement of natural rubber: the use of in situ regenerated cellulose from alkaline–urea–aqueous system, Macromolecules 50 (2017) 7211–7221, https://doi.org/10.1021/acs.macromol.7b01663.
[121] J. Cao, X. Zhang, X. Wu, S. Wang, C. Lu, Cellulose nanocrystals mediated assembly of graphene in rubber composites for chemical sensing applications, Carbohydr. Polym. 140 (2016) 88–95, https://doi.org/10.1016/j.carbpol.2015.12.042.
[122] L. Cao, Z. Gong, C. Xu, Y. Chen, Mechanical strong and recyclable rubber nanocomposites with sustainable cellulose nanocrystals and interfacial exchangeable bonds, ACS Sustain. Chem. Eng. 9 (2021) 9409–9417, https://doi.org/10.1021/acssuschemeng.1c02581.
[123] M. Mariano, N. El Kissi, A. Dufresne, Cellulose nanocrystal reinforced oxidized natural rubber nanocomposites, Carbohydr. Polym. 137 (2016) 174–183, https://doi.org/10.1016/j.carbpol.2015.10.027.
[124] M.G. Thomas, E. Abraham, P. Jyotishkumar, H.J. Maria, L.A. Pothen, S. Thomas, Nanocelluloses from jute fibers and their nanocomposites with natural rubber: preparation and characterization, Int. J. Biol. Macromol. 81 (2015) 768–777, https://doi.org/10.1016/j.ijbiomac.2015.08.053.
[125] S. Singh, G.L. Dhakar, B.P. Kapgate, P.K. Maji, C. Verma, M. Chhajed, K. Rajkumar, C. Das, Synthesis and chemical modification of crystalline nanocellulose to reinforce natural rubber composites, Polym. Adv. Technol. 31 (2020) 3059–3069, https://doi.org/10.1002/pat.5030.
[126] A. Naseem, S. Tabasum, K.M. Zia, M. Zuber, M. Ali, A. Noreen, Lignin-derivatives based polymers, blends and composites: a review, Int. J. Biol. Macromol. 93 (2016) 296–313, https://doi.org/10.1016/j.ijbiomac.2016.08.030.
[127] S. Sen, S. Patil, D.S. Argyropoulos, Thermal properties of lignin in copolymers, blends, and composites: a review, Green Chem. 17 (2015) 4862–4887, https://doi.org/10.1039/C5GC01066G.
[128] O.A.T. Dias, D.R. Negrão, D.F.C. Gonçalves, I. Cesarino, A.L. Leão, Recent approaches and future trends for lignin-based materials, Mol. Cryst. Liq. Cryst. 655 (2017) 204–223, https://doi.org/10.1080/15421406.2017.1360713.
[129] D.S. Argyropoulos, H. Sadeghifar, C. Cui, S. Sen, Synthesis and characterization of poly(arylene ether sulfone) Kraft lignin heat stable copolymers, ACS Sustain. Chem. Eng. 2 (2014) 264–271, https://doi.org/10.1021/sc4002998.
[130] M.R. Ridho, E.A. Agustiany, M. Rahmi Dn, E.W. Madyaratri, M. Ghozali, W. K. Restu, F. Falah, M.A. Rahandi Lubis, F.A. Syamani, Y. Nurhamiyah, et al., Lignin as green filler in polymer composites: development methods, characteristics, and potential applications, Adv. Mater. Sci. Eng. 2022 (2022) 1363481, https://doi.org/10.1155/2022/1363481.
[131] B.M. Upton, A.M. Kasko, Strategies for the conversion of lignin to high-value polymeric materials: review and perspective, Chem. Rev. 116 (2016) 2275–2306, https://doi.org/10.1021/acs.chemrev.5b00345.
[132] N.A. Mohamad Aini, N. Othman, M.H. Hussin, K. Sahakaro, N. Hayeemasae, Lignin as alternative reinforcing filler in the rubber industry: a review, Front Mater 6 (2020) 1–18.
[133] K. Roy, S.C. Debnath, P. Potiyaraj, A review on recent trends and future prospects of lignin based green rubber composites, J. Polym. Environ. 28 (2020) 367–387, https://doi.org/10.1007/s10924-019-01626-5.
[134] D.K. Setua, M.K. Shukla, V. Nigam, H. Singh, G.N. Mathur, Lignin reinforced rubber composites, Polym. Compos. 21 (2000) 988–995, https://doi.org/10.1002/pc.10252.
[135] Mohamad Aini, Nor Anizah, Nadras Othman, Hussin, M. Hazwan, Kannika Sahakaro, N. Hayeemasae, Lignin as alternative reinforcing filler in the rubber industry: a review, Front. Mater. 6 (2020) 329.
[136] P. Yu, H. He, Y. Jia, S. Tian, J. Chen, D. Jia, Y. Luo, A comprehensive study on lignin as a green alternative of silica in natural rubber composites, Polym. Test. 54 (2016) 176–185, https://doi.org/10.1016/j.polymertesting.2016.07.014.
[137] N.A.M. Aini, N. Othman, M.H. Hussin, K. Sahakaro, N. Hayeemasae, Effect of hybrid carbon black/lignin on rheological, mechanical and thermal stability properties of NR/BR composites, Plast. Rubber Compos. 51 (2022) 293–305, https://doi.org/10.1080/14658011.2021.1981718.
[138] N.A. Mohamad Aini, N. Othman, M.H. Hussin, K. Sahakaro, N. Hayeemasae, Efficiency of interaction between hybrid fillers carbon black/lignin with various rubber-based compatibilizer, epoxidized natural rubber, and liquid butadiene rubber in NR/BR composites: mechanical, flexibility and dynamical properties, Ind. Crops Prod. 185 (2022) 115167, https://doi.org/10.1016/j.indcrop.2022.115167.
[139] S. Hait, D. De, A.K. Ghosh, M. Al Aiti, P. Ghosh, J. Chanda, R. Mukhopadhyay, S. Dasgupta, S. Wießner, G. Heinrich, et al., Treasuring waste lignin as superior reinforcing filler in high cis-polybutadiene rubber: a direct comparative study with standard reinforcing silica and carbon black, J. Clean. Prod. 299 (2021) 126841, https://doi.org/10.1016/j.jclepro.2021.126841.
[140] A. Khan, L.K. Kian, M. Jawaid, A.A.P. Khan, H.M. Marwani, M.M. Alotaibi, A. M. Asiri, Preparation and characterization of lignin/nano graphene oxide/styrene butadiene rubber composite for automobile tyre application, Int. J. Biol. Macromol. 206 (2022) 363–370, https://doi.org/10.1016/j.ijbiomac.2022.02.146.
[141] J. Intapun, T. Rungruang, S. Suchat, B. Cherdchim, S. Hiziroglu, The characteristics of natural rubber composites with Klason lignin as a green reinforcing filler: thermal stability, mechanical and dynamical properties, Polymers (Basel) 13 (2021), https://doi.org/10.3390/polym13071109.
[142] A. Hosseinmardi, N. Amiralian, A.N. Hayati, D.J. Martin, P.K. Annamalai, Toughening of natural rubber nanocomposites by the incorporation of nanoscale lignin combined with an industrially relevant leaching process, Ind. Crops Prod. 159 (2021) 113063, https://doi.org/10.1016/j.indcrop.2020.113063.
[143] P. Yu, H. He, C. Jiang, D. Wang, Y. Jia, L. Zhou, D. Jia, Reinforcing styrene butadiene rubber with lignin-novolac epoxy resin networks, Express Polym. Lett. 9 (2015).
[144] C. Jiang, H. He, X. Yao, P. Yu, L. Zhou, D. Jia, In situ dispersion and compatibilization of lignin/epoxidized natural rubber composites: reactivity, morphology and property, J. Appl. Polym. Sci. 132 (2015), https://doi.org/10.1002/app.42044.
[145] C. Jiang, H. He, X. Yao, P. Yu, L. Zhou, D. Jia, The aggregation structure regulation of lignin by chemical modification and its effect on the property of lignin/styrene–butadiene rubber composites, J. Appl. Polym. Sci. 135 (2018) 45759, https://doi.org/10.1002/app.45759.
[146] J. Datta, P. Parcheta, J. Surówka, Softwood-lignin/natural rubber composites containing novel plasticizing agent: preparation and characterization, Ind. Crops Prod. 95 (2017) 675–685, https://doi.org/10.1016/j.indcrop.2016.11.036.
[147] R. Shorey, A. Gupta, T.H. Mekonnen, Hydrophobic modification of lignin for rubber composites, Ind. Crops Prod. 174 (2021) 114189, https://doi.org/10.1016/j.indcrop.2021.114189.
[148] S.C. Saraiva Rodrigues, A.S. da Silva, L.H. de Carvalho, T.S. Alves, R. Barbosa, Morphological, structural, thermal properties of a native starch obtained from babassu mesocarp for food packaging application, J. Mater. Res. Technol. 9 (2020) 15670–15678, https://doi.org/10.1016/j.jmrt.2020.11.030.
[149] T. Spychaj, K. Wilpiszewska, M. Zdanowicz, Medium and high substituted carboxymethyl starch: synthesis, characterization and application, Starch - Stärke 65 (2013) 22–33, https://doi.org/10.1002/star.201200159.
[150] S.-A. Riyajan, S. Patisat, A novel packaging film from cassava starch and natural rubber, J. Polym. Environ. 26 (2018) 2845–2854, https://doi.org/10.1007/s10924-017-1172-5.
[151] C. Liu, Y. Shao, D. Jia, Chemically modified starch reinforced natural rubber composites, Polymer (Guildf). 49 (2008) 2176–2181, https://doi.org/10.1016/j.polymer.2008.03.005.
[152] N.K. Genkina, J. Wikman, E. Bertoft, V.P. Yuryev, Effects of structural imperfection on gelatinization characteristics of amylopectin starches with A- and B-type crystallinity, Biomacromolecules 8 (2007) 2329–2335, https://doi.org/10.1021/bm070349f.
[153] M.A. Misman, A.A. Rashid, S.R. Yahya, Modification and application of starch in natural rubber latex composites, Rubber Chem. Technol. 91 (2018) 184–204, https://doi.org/10.5254/rct-18-82604.
[154] Filomeno Gennaro Corvasce, F.A.J. Fourgon, Preparation of Starch Reinforced Rubber and Use Thereof in Tires, 2007.
[155] J. Wu, K. Li, X. Pan, S. Liao, J. You, K. Zhu, Z. Wang, Preparation and physical properties of porous starch/natural rubber composites, Starch - Stärke 70 (2018) 1700296, https://doi.org/10.1002/star.201700296.
[156] X. Du, Y. Zhang, X. Pan, F. Meng, J. You, Z. Wang, Preparation and properties of modified porous starch/carbon black/natural rubber composites, Compos. Part B Eng. 156 (2019) 1–7, https://doi.org/10.1016/j.compositesb.2018.08.033.

[157] A. Sowińska-Baranowska, M. Maciejewska, P. Duda, The potential application of starch and walnut shells as biofillers for natural rubber (NR) composites, Int. J. Mol. Sci. 23 (2022), https://doi.org/10.3390/ijms23147968.
[158] Raymond D. J.D.E.O. Uzoh, J. Hardy, Macro properties enhancement in natural rubber by polynesian arrow root (amora) starch biofiller through latex compounding method and nanoscale downsizing, African Sch. Publ. Res. Int. 6 (2022).
[159] Y.J. Gao, L. Fang, S. Li, L. Li, S. Liao, Z. Wang, Effect of starch nanocrystal on the properties of carbon black-natural rubber composites, Asian J. Chem. 26 (2014) 5513.
[160] M.M. Senna, R.M. Mohamed, A.N. Shehab-Eldin, S. El-Hamouly, Characterization of electron beam irradiated natural rubber/modified starch composites, J. Ind. Eng. Chem. 18 (2012) 1654–1661, https://doi.org/10.1016/j.jiec.2012.03.004.
[161] M.-C. Li, X. Ge, U.R. Cho, Emulsion grafting vinyl monomers onto starch for reinforcement of styrene-butadiene rubber, Macromol. Res. 21 (2013) 519–528, https://doi.org/10.1007/s13233-013-1052-3.
[162] S. Bhadra, N. Mohan, S. Nair, Suitability of different biomaterials for the application in tire, SN Appl. Sci. 1 (2019) 1554, https://doi.org/10.1007/s42452-019-1625-7.
[163] O.M. Sanusi, A. Benelfellah, N. Aït Hocine, Clays and carbon nanotubes as hybrid nanofillers in thermoplastic-based nanocomposites – a review, Appl. Clay Sci. 185 (2020) 105408, https://doi.org/10.1016/j.clay.2019.105408.
[164] Johannes Lehmann, S. Joseph, Biochar for Environmental Management: Science, Technology and Implementation, Routledge, 2015.
[165] F.N.D. Mukome, X. Zhang, L.C.R. Silva, J. Six, S.J. Parikh, Use of chemical and physical characteristics to investigate trends in biochar feedstocks, J. Agric. Food Chem. 61 (2013) 2196–2204, https://doi.org/10.1021/jf3049142.
[166] A. Demirbas, Effects of temperature and particle size on bio-char yield from pyrolysis of agricultural residues, J. Anal. Appl. Pyrolysis 72 (2004) 243–248, https://doi.org/10.1016/j.jaap.2004.07.003.
[167] W.-J. Liu, H. Jiang, H.-Q. Yu, Development of biochar-based functional materials: toward a sustainable platform carbon material, Chem. Rev. 115 (2015) 12251–12285, https://doi.org/10.1021/acs.chemrev.5b00195.
[168] M. Lay, A. Rusli, M.K. Abdullah, Z.A. Abdul Hamid, R.K. Shuib, Converting dead leaf biomass into activated carbon as a potential replacement for carbon black filler in rubber composites, Compos. Part B Eng. 201 (2020) 108366, https://doi.org/10.1016/j.compositesb.2020.108366.
[169] D.M. Paleri, A. Rodriguez-Uribe, M. Misra, A.K. Mohanty, Preparation and characterization of eco-friendly hybrid biocomposites from natural rubber, biocarbon, and carbon black, Express Polym. Lett. 15 (2021) 236–249.
[170] C. Jiang, J. Bo, X. Xiao, S. Zhang, Z. Wang, G. Yan, Y. Wu, C. Wong, H. He, Converting waste lignin into nano-biochar as a renewable substitute of carbon black for reinforcing styrene-butadiene rubber, Waste Manag 102 (2020) 732–742, https://doi.org/10.1016/j.wasman.2019.11.019.
[171] J. Lubura, O. Kočková, B. Strachota, O. Bera, E. Pavlova, J. Pavličević, B. Ikonić, P. Kojić, A. Strachota, Natural rubber composites using hydrothermally carbonized hardwood waste biomass as a partial reinforcing filler—Part II: mechanical, thermal and ageing (chemical) properties, Polymers (Basel) 15 (2023), https://doi.org/10.3390/polym15102397.
[172] M.E. Abd El-Aziz, E.S. Shafik, M.L. Tawfic, S.M.M. Morsi, Biochar from waste agriculture as reinforcement filer for styrene/butadiene rubber, Polym. Compos. 43 (2022) 1295–1304, https://doi.org/10.1002/pc.26448.
[173] Z. Zainal Abidin, S.N.L. Mamauod, A.Z. Romli, S.S. Sarkawi, N.H. Zainal, Synergistic effect of partial replacement of carbon black by palm kernel shell biochar in carboxylated nitrile butadiene rubber composites, Polymers (Basel) 15 (2023), https://doi.org/10.3390/polym15040943.
[174] S.C. Peterson, S. Kim, Reducing biochar particle size with nanosilica and its effect on rubber composite reinforcement, J. Polym. Environ. 28 (2020) 317–322, https://doi.org/10.1007/s10924-019-01604-x.
[175] S.C. Peterson, Silica-milled Paulownia biochar as partial replacement of carbon black filler in natural rubber, J. Compos. Sci. 3 (2019), https://doi.org/10.3390/jcs3040107.
[176] S.C. Peterson, Coppiced biochars as partial replacement of carbon black filler in polybutadiene/natural rubber composites, J. Compos. Sci. 4 (2020), https://doi.org/10.3390/jcs4040147.
[177] S.C. Peterson, S. Kim, Using heat-treated starch to modify the surface of biochar and improve the tensile properties of biochar-filled styrene–butadiene rubber composites, J. Elastomers \& Plast. 51 (2019) 26–35, https://doi.org/10.1177/0095244318768636.
[178] S.C. Peterson, S.R. Chandrasekaran, B.K. Sharma, Birchwood biochar as partial carbon black replacement in styrene–butadiene rubber composites, J. Elastomers \& Plast. 48 (2016) 305–316, https://doi.org/10.1177/0095244315576241.
[179] M.-C. Li, Y. Zhang, U.R. Mechanical Cho, Thermal and friction properties of rice bran carbon/nitrile rubber composites: influence of particle size and loading, Mater. Des. 63 (2014) 565–574, https://doi.org/10.1016/j.matdes.2014.06.032.
[180] X. Meng, Y. Zhang, J. Lu, Z. Zhang, L. Liu, P.K. Chu, Effect of bamboo charcoal powder on the curing characteristics, mechanical properties, and thermal properties of styrene–butadiene rubber with bamboo charcoal powder, J. Appl. Polym. Sci. 130 (2013) 4534–4541, https://doi.org/10.1002/app.39522.
[181] S.C. Peterson, Evaluating corn starch and corn stover biochar as renewable filler in carboxylated styrene–butadiene rubber composites, J. Elastomers \& Plast. 44 (2012) 43–54, https://doi.org/10.1177/0095244311414011.
[182] J. Shi, H. Zou, L. Ding, X. Li, K. Jiang, T. Chen, X. Zhang, L. Zhang, D. Ren, Continuous production of liquid reclaimed rubber from ground tire rubber and its application as reactive polymeric plasticizer, Polym. Degrad. Stab. 99 (2014) 166–175, https://doi.org/10.1016/j.polymdegradstab.2013.11.010.
[183] D. Mondal, S. Hait, S. Ghorai, S. Wießner, A. Das, D. De, D. Chattopadhyay, Back to the origin: a spick-and-span sustainable approach for the devulcanization of ground tire rubber, J. Vinyl Addit. Technol. 29 (2023) 240–258, https://doi.org/10.1002/vnl.21974.
[184] C. Sathiskumar, S. Karthikeyan, Recycling of waste tires and its energy storage application of by-products –a review, Sustain. Mater. Technol. 22 (2019) e00125, https://doi.org/10.1016/j.susmat.2019.e00125.
[185] C. Dwivedi, S. Manjare, S.K. Rajan, Recycling of waste tire by pyrolysis to recover carbon black: alternative & environment-friendly reinforcing filler for natural rubber compounds, Compos. Part B Eng. 200 (2020) 108346, https://doi.org/10.1016/j.compositesb.2020.108346.
[186] M. Nuzaimah, S.M. Sapuan, R. Nadlene, M. Jawaid, Recycling of waste rubber as fillers: a review, IOP Conf. Ser. Mater. Sci. Eng. 368 (2018) 12016, https://doi.org/10.1088/1757-899X/368/1/012016.
[187] G. Zhang, Y. Jiang, S. Wang, Y. Zhang, Influence of a novel coupling agent on the performance of recovered carbon black filled natural rubber, Compos. Part B Eng. 255 (2023) 110614, https://doi.org/10.1016/j.compositesb.2023.110614.
[188] Y. Song, G. Wu, D. Wang, J. Peng, C. Zhang, Q. Zheng, Tailoring reinforcement and strain softening behaviors of natural rubber vulcanizates nanocomposites by dopamine-modified silica, Compos. Part B Eng. 254 (2023) 110552, https://doi.org/10.1016/j.compositesb.2023.110552.
[189] J. Araujo-Morera, R. Verdugo-Manzanares, S. González, R. Verdejo, M.A. Lopez-Manchado, M. Hernández Santana, On the use of mechano-chemically modified ground tire rubber (GTR) as recycled and sustainable filler in styrene-butadiene rubber (SBR) composites, J. Compos. Sci. 5 (2021), https://doi.org/10.3390/jcs5030068.
[190] M. Jovičić, O. Bera, S. Stojanov, J. Pavličević, D. Govedarica, I. Bobinac, B. B. Hollo, Effects of recycled carbon black generated from waste rubber on the curing process and properties of new natural rubber composites, Polym. Bull. 80 (2023) 5047–5069, https://doi.org/10.1007/s00289-022-04307-x.
[191] S. Ghorai, S. Hait, D. Mondal, S. Wießner, A. Das, D. De, Fill two needs with one deed: simultaneous devulcanization and silica reinforcement of waste rubber for green tyre tread compound, Mater. Today Commun. 35 (2023) 106065, https://doi.org/10.1016/j.mtcomm.2023.106065.
[192] X. Tian, Q. Zhuang, S. Han, S. Li, H. Liu, L. Li, J. Zhang, C. Wang, H. Bian, A novel approach of reapplication of carbon black recovered from waste tyre pyrolysis to rubber composites, J. Clean. Prod. 280 (2021) 124460, https://doi.org/10.1016/j.jclepro.2020.124460.
[193] G. Zhang, Y. Zhang, S. Wang, Y. Jiang, Effect of pyrolysis carbon black from waste tire on the mechanical properties of SSBR/BR blend, Macromol. Mater. Eng. 307 (2022) 2100944, https://doi.org/10.1002/mame.202100944.